The Lagrangian Solutions

Àngel Jorba

Departament de Matemàtica Aplicada i Anàlisi

Universitat de Barcelona

Gran Via 585, 08007 Barcelona, Spain

E-mail: `<angel@maia.ub.es>`

December 1st, 2012

Abstract

This chapter focuses on the dynamics in a neighbourhood of the five equilibrium points of the Restricted Three-Body Problem. The first section is devoted to the discussion of the linear behaviour near the five points. Then, the motion in the vicinity of the collinear points is considered, discussing the effective computation of the center manifold as a tool to describe the nonlinear dynamics in an extended neigbourhood of these points. This technique is then applied to the Earth-Moon case, showing the existence of periodic and quasi-periodic motions, including the well-known Halo orbits. Next, the dynamics near the triangular points is discussed, showing how normal forms can be used to effectively describe the motion nearby. The Lyapunov stability is also considered, showing how the stability is proved in the planar case, and why it is not proved in the spatial case. This section also discusses how to bound the amount of diffusion that could be present in the spatial case. Finally, in the last section we focus on the effect of perturbations. More concretely, we mention the Elliptic Restricted Three-Body Problem, the Bicircular problem and similar models that contain periodic and quasi-periodic time-dependent perturbations.

Contents

1 Introduction

Let us consider two point masses (usually called primaries) that attract each other according to the gravitational Newton's law. Let us assume that they are moving in circular orbits around their common centre of mass, and let us consider the motion of an infinitesimal particle (here, infinitesimal means that its mass is so small that we neglect the effect it has on the motion of the primaries and we only take into account the effect of the primaries on the particle) under the attraction of the two primaries. The study of the motion of the infinitesimal particle is what is known as the Restricted Three-Body Problem, or RTBP for short.

To simplify the equations of motion, let us take units of mass, length and time such that the sum of masses of the primaries, the gravitational constant and the period of the motion of the primaries are 1, 1 and 2π respectively. With these units the distance between the primaries is also equal to 1. We denote as μ the mass of the smaller primary (the mass of the bigger is then $1 - \mu$), $\mu \in (0, \frac{1}{2}]$.

The usual system of reference is defined as follows: the origin is taken at the centre of mass of the primaries, the X-axis points to the bigger primary, the Z-axis is perpendicular to the plane of motion, pointing in the same direction as the vector of angular momentum of the primaries with respect to their common centre of mass, and the Y-axis is defined such that we obtain an orthogonal, positive-oriented system of reference. With this we have defined a rotating system of reference, that is usually called synodic. In this system, the primary of mass μ is located at the point $(\mu - 1, 0, 0)$ and the one of mass $1 - \mu$ is located at $(\mu, 0, 0)$, see Figure 1.

Defining momenta as $P_X = \dot{X} - Y$, $P_Y = \dot{Y} + X$ and $P_Z = \dot{Z}$, the equations of motion can be written in Hamiltonian form. The corresponding Hamiltonian function is

$$H = \frac{1}{2}(P_X^2 + P_Y^2 + P_Z^2) + Y P_X - X P_Y - \frac{1 - \mu}{r_1} - \frac{\mu}{r_2}, \tag{1}$$

being $r_1^2 = (X - \mu)^2 + Y^2 + Z^2$ and $r_2^2 = (X - \mu + 1)^2 + Y^2 + Z^2$ (see, for instance, [78] for the details).

It is well-known that the system defined by (1) has five equilibrium points. Two of them can be found as the third vertex of the two equilateral triangles that can be formed using the two primaries as vertices (usually called $L_{4,5}$ or Lagrangian points). The other three lie on the X-axis and are usually called $L_{1,2,3}$ or Eulerian points (see Figure 1). A more detailed discussion on the existence of these points can be found in many textbooks, like [78]. Note that "our" L_1 and L_2 are swapped with respect to that reference. This lack of agreement for the definition of $L_{1,2}$ is rather common in the literature: usually, books on celestial mechanics use the same notation as in [78] but books on astrodynamics follow the convention we use here.

In this chapter we will focus on the dynamics around these points, specially for examples coming from the Solar system. We will also comment on the main perturbations that appear in astronomical and astronautical applications and their effects.
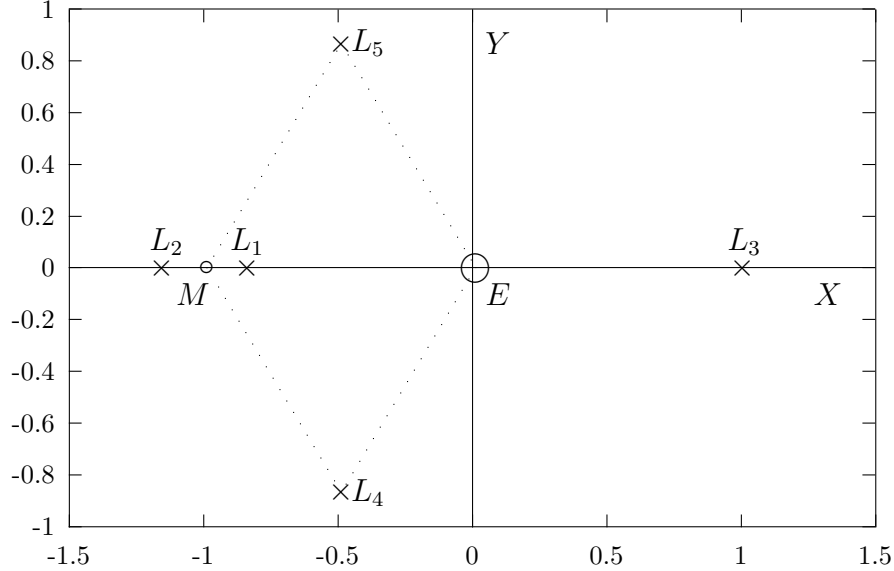
Figure 1: The five equilibrium points of the RTBP. The graphic corresponds to the Earth-Moon case. The unit of distance is the Earth-Moon distance, and the unit of mass is the total mass of the system. In these units, the mass of the Moon is $\mu \approx 0.01215$.

2   Linear behaviour

In this section we will first discuss the linearization of the dynamics around the five equilibrium points. The presentation is done in a way that prepares the following sections.

2.1   The collinear points

Let us define, for $j = 1, 2$, γ_j as the distance from the smaller primary (the one of mass μ) to the point L_j, and γ_3 as the distance from the bigger primary to L_3. It is well-known (see, for instance, [78]) that γ_j is the only positive solution of the Euler quintic equation,

$$\gamma_j^5 \mp (3 - \mu)\gamma_j^4 + (3 - 2\mu)\gamma_j^3 - \mu\gamma_j^2 \pm 2\mu\gamma_j - \mu = 0, \quad j = 1, 2,$$
$$\gamma_3^5 + (2 + \mu)\gamma_3^4 + (1 + 2\mu)\gamma_3^3 - (1 - \mu)\gamma_3^2 - 2(1 - \mu)\gamma_3 - (1 - \mu) = 0,$$

where the upper sign in the first equation is for L_1 and the lower one for L_2. These equations can be solved numerically by the Newton method, using the starting point $(\mu/3)^{1/3}$ for the first equation ($L_{1,2}$ cases), and $1 - \frac{7}{12}\mu$ for the second one (L_3 case).

The next step is to translate the origin to the selected point L_j. Moreover, since in Section 3 we will need the power expansion of the Hamiltonian at these points, we therefore perform a suitable scaling in order to avoid fast growing (or decreasing) coefficients. The idea is to have the closest singularity (the body of mass μ for $L_{1,2}$ or the one of mass $1 - \mu$ for L_3) at distance 1 (see [68]). As the scalings are not symplectic transformations,

let us consider the following process: first we write the differential equations related to (1) and then, on these equations, we perform the following substitution

$$
\begin{aligned}
X &= \mp\gamma_j x + \mu + \alpha_j, \\
Y &= \mp\gamma_j y, \\
Z &= \gamma_j z,
\end{aligned}
$$

where the upper sign corresponds to $L_{1,2}$, the lower one to L_3 and $\alpha_1 = -1 + \gamma_1$, $\alpha_2 = -1 - \gamma_2$ and $\alpha_3 = \gamma_3$. Note that the unit of distance is now the distance from the equilibrium point to the closest primary.

In order to expand the nonlinear terms, we will use that

$$
\frac{1}{\sqrt{(x-A)^2 + (y-B)^2 + (z-C)^2}} = \frac{1}{D} \sum_{n=0}^{\infty} \left(\frac{\rho}{D}\right)^n P_n\left(\frac{Ax + By + Cz}{D\rho}\right),
$$

where A, B, C, D, are real numbers with $D^2 = A^2 + B^2 + C^2$, $\rho^2 = x^2 + y^2 + z^2$ and P_n is the polynomial of Legendre of degree n. After some calculations, one obtains that the equations of motion can be written as

$$
\begin{aligned}
\ddot{x} - 2\dot{y} - (1 + 2c_2)x &= \frac{\partial}{\partial x} \sum_{n\geq 3} c_n(\mu)\rho^n P_n\left(\frac{x}{\rho}\right), \\
\ddot{y} + 2\dot{x} + (c_2 - 1)y &= \frac{\partial}{\partial y} \sum_{n\geq 3} c_n(\mu)\rho^n P_n\left(\frac{x}{\rho}\right), \qquad\qquad (2) \\
\ddot{z} + c_2 z &= \frac{\partial}{\partial z} \sum_{n\geq 3} c_n(\mu)\rho^n P_n\left(\frac{x}{\rho}\right),
\end{aligned}
$$

where the left-hand side contains the linear terms and the right-hand side contains the nonlinear ones. The coefficients $c_n(\mu)$ are given by

$$
\begin{aligned}
c_n(\mu) &= \frac{1}{\gamma_j^3} \left((\pm 1)^n \mu + (-1)^n \frac{(1-\mu)\gamma_j^{n+1}}{(1 \mp \gamma_j)^{n+1}} \right), \qquad \text{for } L_j, \; j = 1, 2 \\
c_n(\mu) &= \frac{(-1)^n}{\gamma_3^3} \left(1 - \mu + \frac{\mu\gamma_3^{n+1}}{(1+\gamma_3)^{n+1}} \right), \qquad \text{for } L_3.
\end{aligned}
$$

In the first equation, the upper sign is for L_1 and the lower one for L_2. Note that these equations can be written in Hamiltonian form, by defining the momenta $p_x = \dot{x} - y$, $p_y = \dot{y} + x$ and $p_z = \dot{z}$. The corresponding Hamiltonian is then given by

$$
H = \frac{1}{2}\left(p_x^2 + p_y^2 + p_z^2\right) + yp_x - xp_y - \sum_{n\geq 2} c_n(\mu)\rho^n P_n\left(\frac{x}{\rho}\right). \qquad\qquad (3)
$$

The nonlinear terms of this Hamiltonian can be expanded by means of the well-known recurrence of the Legendre polynomials P_n. For instance, if we define

$$
T_n(x, y, z) = \rho^n P_n\left(\frac{x}{\rho}\right), \qquad\qquad (4)
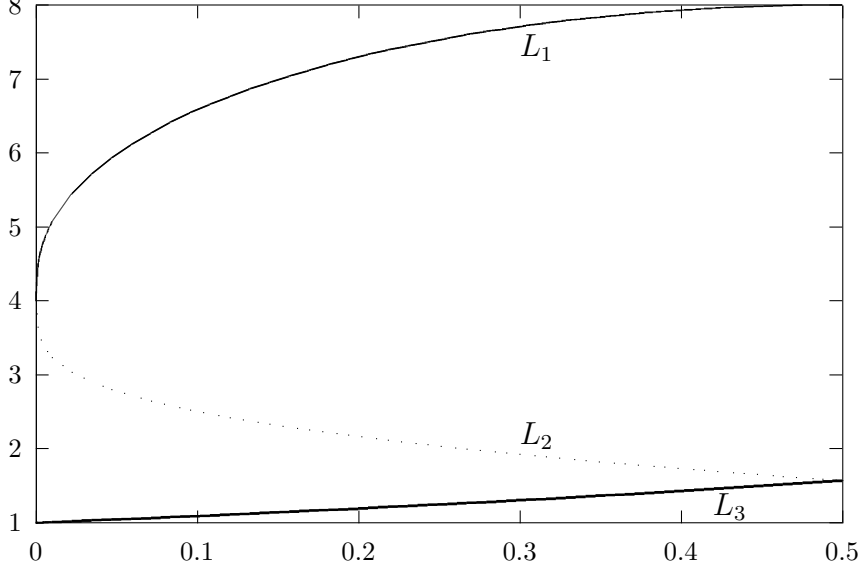$$

Figure 2: Values of $c_2(\mu)$ (vertical axis), for $\mu \in [0, \frac{1}{2}]$ (horizontal axis), for the cases $L_{1,2,3}$.

then, it is not difficult to check that T_n is a homogeneous polynomial of degree n that satisfies the recurrence

$$T_n = \frac{2n-1}{n} x T_{n-1} - \frac{n-1}{n} (x^2 + y^2 + z^2) T_{n-2}, \tag{5}$$

starting with $T_0 = 1$ and $T_1 = x$.

The linearization around the equilibrium point is given by the second order terms of the Hamiltonian (linear terms must vanish) that, after some rearranging, take the form,

$$H_2 = \frac{1}{2} \left(p_x^2 + p_y^2 \right) + y p_x - x p_y - c_2 x^2 + \frac{c_2}{2} y^2 + \frac{1}{2} p_z^2 + \frac{c_2}{2} z^2. \tag{6}$$

It is not difficult to derive intervals for the values of $c_2 = c_2(\mu)$ when $\mu \in [0, \frac{1}{2}]$ (see Figure 2). As $c_2 > 0$ (for the three collinear points), the vertical direction is an harmonic oscillator with frequency $\omega_2 = \sqrt{c_2}$. Now let us focus on the planar directions, i.e.,

$$H_2 = \frac{1}{2} \left(p_x^2 + p_y^2 \right) + y p_x - x p_y - c_2 x^2 + \frac{c_2}{2} y^2, \tag{7}$$

where, for simplicity, we keep the name H_2 for the Hamiltonian.

Now, let us define the matrix M as $J\text{Hess}(H_2)$,

$$M = \begin{pmatrix} 0 & 1 & 1 & 0 \\ -1 & 0 & 0 & 1 \\ 2c_2 & 0 & 0 & 1 \\ 0 & -c_2 & -1 & 0 \end{pmatrix}. \tag{8}$$

6

The characteristic polynomial is $p(\lambda) = \lambda^4 + (2 - c_2)\lambda^2 + (1 + c_2 - 2c_2^2)$. Calling $\eta = \lambda^2$, we have that the roots of $p(\lambda) = 0$ are given by

$$\eta_1 = \frac{c_2 - 2 - \sqrt{9c_2^2 - 8c_2}}{2}, \qquad \eta_2 = \frac{c_2 - 2 + \sqrt{9c_2^2 - 8c_2}}{2}.$$

As $\mu \in]0, \frac{1}{2}]$ we have that $c_2 > 1$ that forces $\eta_1 < 0$ and $\eta_2 > 0$. This shows that the equilibrium point is a centre×centre×saddle. Thus, let us define ω_1 as $\sqrt{-\eta_1}$ and λ_1 as $\sqrt{\eta_2}$. For the moment, we do not specify the sign taken for each value (this will be discussed later on).

Now, we want to find a symplectic linear change of variables casting (7) into its real normal form (by real we mean with real coefficients) and, hence, we will look for the eigenvectors of matrix (8). As usual, we will take advantage of the special form of this matrix: if we denote by M_λ the matrix $M - \lambda I_4$, then

$$M_\lambda = \begin{pmatrix} A_\lambda & I_2 \\ B & A_\lambda \end{pmatrix}, \qquad A_\lambda = \begin{pmatrix} -\lambda & 1 \\ -1 & -\lambda \end{pmatrix}, \qquad B = \begin{pmatrix} 2c_2 & 0 \\ 0 & -c_2 \end{pmatrix}.$$

Now, the kernel of M_λ can be found as follows: denoting as $(w_1^\top, w_2^\top)^\top$ the elements of the kernel, we start solving $(B - A^2)w_1 = 0$ and then $w_2 = -Aw_1$. Thus, the eigenvectors of M are given by $(2\lambda, \lambda^2 - 2c_2 - 1, \lambda^2 + 2c_2 + 1, \lambda^3 + (1 - 2c_2)\lambda)^\top$, where λ denotes the eigenvalue.

Let us consider now the eigenvectors related to ω_1. From $p(\lambda) = 0$, we obtain that ω_1 verifies

$$\omega_1^4 - (2 - c_2)\omega_1^2 + (1 + c_2 - 2c_2^2) = 0.$$

We also apply $\lambda = \sqrt{-1}\omega_1$ to the expression of the eigenvector and, separating real and imaginary parts as $u_{\omega_1} + \sqrt{-1}v_{\omega_1}$ we obtain

$$\begin{aligned} u_{\omega_1} &= (0, -\omega_1^2 - 2c_2 - 1, -\omega_1^2 + 2c_2 + 1, 0)^\top, \\ v_{\omega_1} &= (2\omega_1, 0, 0, -\omega_1^3 + (1 - 2c_2)\omega_1)^\top. \end{aligned}$$

Now, let us consider the eigenvalues related to $\pm\lambda_1$,

$$\begin{aligned} u_{+\lambda_1} &= (2\lambda, \lambda^2 - 2c_2 - 1, \lambda^2 + 2c_2 + 1, \lambda^3 + (1 - 2c_2)\lambda)^\top, \\ v_{-\lambda_1} &= (-2\lambda, \lambda^2 - 2c_2 - 1, \lambda^2 + 2c_2 + 1, -\lambda^3 - (1 - 2c_2)\lambda)^\top. \end{aligned}$$

We consider, initially, the change of variables $C = (u_{+\lambda_1}, u_{\omega_1}, v_{-\lambda_1}, v_{\omega_1})$. To know whether this matrix is symplectic or not, we check $C^\top JC = J$. It is a tedious computation to see that

$$C^\top JC = \begin{pmatrix} 0 & D \\ -D & 0 \end{pmatrix}, \qquad D = \begin{pmatrix} d_{\lambda_1} & 0 \\ 0 & d_{\omega_1} \end{pmatrix}.$$

This implies that we need to apply some scaling on the columns of C in order to have a symplectic change. The scaling is given by the factors

$$d_{\lambda_1} = 2\lambda_1((4 + 3c_2)\lambda_1^2 + 4 + 5c_2 - 6c_2^2), \qquad d_{\omega_1} = \omega_1((4 + 3c_2)\omega_1^2 - 4 - 5c_2 + 6c_2^2).$$

Thus, we define $s_1 = \sqrt{d_{\lambda_1}}$ and $s_2 = \sqrt{d_{\omega_1}}$. As we want the change to be real, we have to require $d_{\lambda_1} > 0$ and $d_{\omega_1} > 0$. It is not difficult to check that this condition is satisfied for $0 < \mu \leq \frac{1}{2}$ in all the points $L_{1,2,3}$, if $\lambda_1 > 0$ and $\omega_1 > 0$.

To obtain the final change, we have to take into account the vertical direction (z, p_z): to put it into real normal form we use the substitution

$$z \mapsto \frac{1}{\sqrt{\omega_2}} z, \qquad p_z \mapsto \sqrt{\omega_2} p_z.$$

This implies that the final change is given by the symplectic matrix

$$C = \begin{pmatrix} \frac{2\lambda}{s_1} & 0 & 0 & \frac{-2\lambda}{s_1} & \frac{2\omega_1}{s_2} & 0 \\ \frac{\lambda^2 - 2c_2 - 1}{s_1} & \frac{-\omega_1^2 - 2c_2 - 1}{s_2} & 0 & \frac{\lambda^2 - 2c_2 - 1}{s_1} & 0 & 0 \\ 0 & 0 & \frac{1}{\sqrt{\omega_2}} & 0 & 0 & 0 \\ \frac{\lambda^2 + 2c_2 + 1}{s_1} & \frac{-\omega_1^2 + 2c_2 + 1}{s_2} & 0 & \frac{\lambda^2 + 2c_2 + 1}{s_1} & 0 & 0 \\ \frac{\lambda^3 + (1 - 2c_2)\lambda}{s_1} & 0 & 0 & \frac{-\lambda^3 - (1 - 2c_2)\lambda}{s_1} & \frac{-\omega_1^3 + (1 - 2c_2)\omega_1}{s_2} & 0 \\ 0 & 0 & 0 & 0 & 0 & \sqrt{\omega_2} \end{pmatrix} \tag{9}$$

that casts Hamiltonian (6) into its real normal form,

$$H_2 = \lambda_1 x p_x + \frac{\omega_1}{2}(y^2 + p_y^2) + \frac{\omega_2}{2}(z^2 + p_z^2), \tag{10}$$

where, for simplicity, we have kept the same name for the variables. Later on, to simplify the computations, we will use a complex normal form for H_2 because it will simplify the computations. This complexification is given by

$$\begin{array}{llll} x &=& q_1, & y &=& \frac{q_2 + \sqrt{-1} p_2}{\sqrt{2}}, & z &=& \frac{q_3 + \sqrt{-1} p_3}{\sqrt{2}}, \\ p_x &=& p_1, & p_y &=& \frac{\sqrt{-1} q_2 + p_2}{\sqrt{2}}, & p_z &=& \frac{\sqrt{-1} q_3 + p_3}{\sqrt{2}}, \end{array} \tag{11}$$

and it puts (10) into its complex normal form,

$$H_2 = \lambda_1 q_1 p_1 + \sqrt{-1}\,\omega_1 q_2 p_2 + \sqrt{-1}\,\omega_2 q_3 p_3, \tag{12}$$

being λ_1, ω_1 and ω_2 real (and positive) numbers.

2.2 The equilateral points

The equilibrium points L_4 and L_5 are located at $(\mu - \frac{1}{2}, \mp\frac{\sqrt{3}}{2}, 0)$, where the upper ("$-$") sign is for L_4 while the lower ("$+$") one is for L_5. These points are known to be linearly stable when the value of the mass parameter μ is below the Routh critical value $\mu_R = \frac{1}{2}\left(1 - \frac{\sqrt{69}}{9}\right) \approx 0.03852$. In what follows we assume that the value of our mass parameter is less than μ_R. The dynamics for values of μ larger than the Routh critical value will not be discussed here. For more details, you can read [50, 42, 64, 73, 66] and references therein.

The first step is to translate the origin of coordinates to the equilibrium point (note that here we do not need any scaling, since the two masses are already at distance one from the points $L_{4,5}$). The translation is given by the (symplectic) change

$$
\begin{array}{llll}
X &=& x + \mu - \frac{1}{2}, & P_X &=& p_x \pm \frac{\sqrt{3}}{2}, \\
Y &=& y \mp \frac{\sqrt{3}}{2}, & P_Y &=& p_y + \mu - \frac{1}{2}, \\
Z &=& z, & P_Z &=& z,
\end{array}
$$

to the Hamiltonian (1). As before, the upper sign is for L_4 and the lower one for L_5 (this rule for the signs will be used along this section). To simplify notation we use the same symbol H for the Hamiltonian obtained,

$$
H = \frac{1}{2}(p_x^2 + p_y^2 + p_z^2) + yp_x - xp_y + \left(\frac{1}{2} - \mu\right)x \mp \frac{\sqrt{3}}{2}y - \frac{1-\mu}{r_{PS}} - \frac{\mu}{r_{PJ}},
$$

where $r_{PS}^2 = (x - x_S)^2 + (y - y_S)^2 + z^2$, $r_{PJ}^2 = (x - x_J)^2 + (y - y_J)^2 + z^2$, $x_S = 1/2$, $y_S = \mp\sqrt{3}/2$, $x_J = -1/2$ and $y_J = \mp\sqrt{3}/2$. Note that $(x_S, y_S, 0)$ are the coordinates of the big primary in the new coordinates and that $(x_J, y_J, 0)$ is the position of the small one. The subscripts usually correspond to "Sun" and "Jupiter". They provide a classical example for the RTBP, where the small particle can be an asteroid.

The next step is to expand H around the origin. The expansion of the nonlinear terms is performed in the same way as we did in Section 2.1, so we will not repeat the details here. Note that, as the origin is an equilibrium point, the first order terms must vanish (we forget about the constant value $H(0)$, since it is irrelevant to the dynamics). The first non-trivial terms are of second order and they are responsible for the linear dynamics around the point. They are

$$
H_2 = \frac{1}{2}(p_x^2 + p_y^2 + p_z^2) + yp_x - xp_y + \frac{1}{8}x^2 - \frac{5}{8}y^2 - axy + \frac{1}{2}z^2,
$$

where $a = \pm\frac{3\sqrt{3}}{4}(1 - 2\mu)$. Note that the behaviour in the (z, p_z) directions is uncoupled of the behaviour in the (x, y, p_x, p_y) directions. Moreover, the motion on the z-axis corresponds to an harmonic oscillator with frequency 1 (for all μ), that is already in (real) normal form. Hence, we restrict ourselves to the (x, y, p_x, p_y)-plane:

$$
H_2 = \frac{1}{2}(p_x^2 + p_y^2) + yp_x - xp_y + \frac{1}{8}x^2 - \frac{5}{8}y^2 - axy. \tag{13}
$$

Let us define the 4×4 matrix J as

$$
J = \begin{pmatrix} 0 & I_2 \\ -I_2 & 0 \end{pmatrix},
$$

where I_2 denote the 2×2 identity matrix. The equations of motion of (13) are given by the linear system

$$
\begin{pmatrix} \dot{x} \\ \dot{y} \\ \dot{p}_x \\ \dot{p}_y \end{pmatrix} = J\nabla H_2 = J\mathrm{Hess}(H_2) \begin{pmatrix} x \\ y \\ p_x \\ p_y \end{pmatrix}. \tag{14}
$$

9

An easy computation shows that the matrix $M = J\text{Hess}(H_2)$ is given by

$$M = \begin{pmatrix} 0 & 1 & 1 & 0 \\ -1 & 0 & 0 & 1 \\ -\frac{1}{4} & a & 0 & 1 \\ a & \frac{5}{4} & -1 & 0 \end{pmatrix}. \tag{15}$$

The characteristic polynomial is $p(\lambda) = \lambda^4 + \lambda^2 + \frac{27}{16} - a^2$. From this expression it is easy to obtain that system (14) is stable if $\mu \leq \mu_R = \frac{1}{2}\left(1 - \sqrt{\frac{23}{27}}\right)$ (this is the Routh mass) and unstable if $\mu_r < \mu \leq \frac{1}{2}$. As we are studying the case $\mu < \mu_R$, we assume that the solutions of $p(\lambda) = 0$ are all purely imaginary, that is, $\lambda_j = \pm\omega_j\sqrt{-1}$, $j = 1, 2$. The real values ω_j are the frequencies of the linear oscillations at the equilibrium points $L_{4,5}$, and it is trivial to show that they always differ when $0 < \mu < \mu_R$. Let us call ω_1 the one that satisfies $\omega_1^2 > \frac{1}{2}$ and ω_2 the one such that $\omega_2^2 < \frac{1}{2}$. For the moment we do not specify the sign we take for each frequency. These signs will be determined below.

Now we want to obtain a real (and symplectic) change of variables such that the Hamiltonian (13) is reduced to its (real) normal form. The first step will be to look for the eigenvectors of the matrix M given by (15). To simplify the computation, we will take advantage of the special form of this matrix. We denote by M_λ the matrix $M - \lambda I_4$, and we define the following splitting in 2×2 blocks:

$$M_\lambda = \begin{pmatrix} A_\lambda & I_2 \\ B & A_\lambda \end{pmatrix}, \qquad A_\lambda = \begin{pmatrix} -\lambda & 1 \\ -1 & -\lambda \end{pmatrix}, \qquad B = \begin{pmatrix} -\frac{1}{4} & a \\ a & \frac{5}{4} \end{pmatrix}.$$

Here, λ denotes one of the eigenvalues of the matrix M. The kernel of M_λ is now easy to find: to solve

$$\begin{pmatrix} A_\lambda & I_2 \\ B & A_\lambda \end{pmatrix}\begin{pmatrix} w_1 \\ w_2 \end{pmatrix} = \begin{pmatrix} 0 \\ 0 \end{pmatrix},$$

we can start by solving $(B - A^2)w_1 = 0$ and then $w_2 = -Aw_1$ (note that the kernel of $(B - A^2)$ is trivial to find since it is a 2×2 matrix). In this way, we find the eigenvector $(2\lambda + a, \lambda^2 - \frac{3}{4}, \lambda^2 + a\lambda + \frac{3}{4}, \lambda^3 + \frac{5}{4}\lambda + a)^\top$. Now, as the eigenvalues of M satisfy $\lambda = \sqrt{-1}\omega$, $\omega \in \mathbb{R}$, we obtain that the frequencies ω are determined by the equation

$$\omega^4 - \omega^2 + \frac{27}{16} - a^2 = 0. \tag{16}$$

We also apply $\lambda = \sqrt{-1}\omega$ to the expression of the eigenvector and, separating real and imaginary parts, we obtain that it can be expressed as $u + \sqrt{-1}v$, where

$$\left.\begin{array}{rcl} u(\omega) & = & \left(a, -\omega^2 - \frac{3}{4}, -\omega^2 + \frac{3}{4}, a\right)^\top \\ v(\omega) & = & \left(2\omega, 0, a\omega, -\omega^3 + \frac{5}{4}\omega\right)^\top \end{array}\right\}. \tag{17}$$

We start considering the change of variables given by the matrix $C = (u_1, u_2, v_1, v_2)$, where u_j and v_j denote the values of u and v given by (17) corresponding to the frequencies ω_j, $j = 1, 2$. For the moment we do not specify which sign is taken for each frequency.

In order to know whether C is symplectic or not, we check the property $C^\top JC = J$: a tedious but not difficult computation produces

$$C^\top JC = \begin{pmatrix} 0 & D \\ -D & 0 \end{pmatrix}, \quad D = \begin{pmatrix} d(\omega_1) & 0 \\ 0 & d(\omega_2) \end{pmatrix}.$$

where $d(\omega) = \omega(2\omega^4 + \frac{1}{2}\omega^2 - \frac{3}{4})$. Of course, to derive this expression you need to use the properties (16) and $\omega_1^2\omega_2^2 = \frac{27}{16} - a^2$. Note that the zeros obtained in $C^\top JC$ and D were expected, due to the way we have constructed C. The only question was to know whether d is 1 or not. As it is not, we need to perform some scaling to the columns of C: let us define $s_j = \sqrt{d(\omega_j)}$, $j = 1, 2$ and let us redefine C as $(\frac{u_1}{s_1}, \frac{u_2}{s_2}, \frac{v_1}{s_1}, \frac{v_2}{s_2})$. This matrix is now symplectic, but we also want C to be real, that is, we want the values $d(\omega_j)$ to be positive. This will determine the signs we must choose for the frequencies ω_j. As $\omega_1^2 < \frac{1}{2}$, if one wants $d(\omega_1) > 0$ is necessary to take $\omega_1 > 0$ and, conversely, as $\omega_2^2 < \frac{1}{2}$ implies that we must take $\omega_2 < 0$ in order to have $d(\omega_2) > 0$. Hence, the change we have obtained is real, symplectic and it brings the Hamiltonian (13) into the real normal form

$$H_2 = \frac{\omega_1}{2}(x^2 + p_x^2) + \frac{\omega_2}{2}(y^2 + p_y^2), \tag{18}$$

where we recall that $\omega_1 > 0$ and $\omega_2 < 0$.

As in Section 2.1, we want a complex normal form for H_2, because it will simplify the computations in the following sections. So, it is not difficult to derive the change that brings (18) into complex normal form: we compose the complexifying change

$$\begin{array}{rclcrcl}
x & = & \frac{q_1 + \sqrt{-1}p_1}{\sqrt{2}}, & & y & = & \frac{q_2 + \sqrt{-1}p_2}{\sqrt{2}}, \\
p_x & = & \frac{\sqrt{-1}q_1 + p_1}{\sqrt{2}}, & & p_y & = & \frac{\sqrt{-1}q_2 + p_2}{\sqrt{2}},
\end{array}$$

with the above-defined matrix C to produce the final change used in the paper:

$$\begin{pmatrix}
\frac{a}{r_1} + \frac{2\omega_1}{r_1}\sqrt{-1} & \frac{2\omega_1}{r_1} + \frac{a}{r_1}\sqrt{-1} & \frac{a}{r_2} + \frac{2\omega_2}{r_2}\sqrt{-1} & \frac{2\omega_2}{r_2} + \frac{a}{r_2}\sqrt{-1} \\
\frac{-\omega_1^2 - \frac{3}{4}}{r_1} & \frac{-\omega_1^2 - \frac{3}{4}}{r_1}\sqrt{-1} & \frac{-\omega_2^2 - \frac{3}{4}}{r_2} & \frac{-\omega_2^2 - \frac{3}{4}}{r_2}\sqrt{-1} \\
\frac{-\omega_1^2 + \frac{3}{4}}{r_1} + \frac{a\omega_1}{r_1}\sqrt{-1} & \frac{a\omega_1}{r_1} + \frac{-\omega_1^2 + \frac{3}{4}}{r_1}\sqrt{-1} & \frac{-\omega_2^2 + \frac{3}{4}}{r_2} + \frac{a\omega_2}{r_2}\sqrt{-1} & \frac{a\omega_2}{r_2} + \frac{-\omega_2^2 + \frac{3}{4}}{r_2}\sqrt{-1} \\
\frac{a}{r_1} + \frac{-\omega_1^3 + \frac{5}{4}\omega_1}{r_1}\sqrt{-1} & \frac{-\omega_1^3 + \frac{5}{4}\omega_1}{r_1} + \frac{a}{r_1}\sqrt{-1} & \frac{a}{r_2} + \frac{-\omega_2^3 + \frac{5}{4}\omega_2}{r_2}\sqrt{-1} & \frac{-\omega_2^3 + \frac{5}{4}\omega_2}{r_2} + \frac{a}{r_2}\sqrt{-1}
\end{pmatrix},$$

where

$$r_j = \sqrt{\omega_j\left(4\omega_j^4 + \omega_j^2 - \frac{3}{2}\right)}, \quad j = 1, 2.$$

3   Nonlinear dynamics near the collinear points

We have already seen that the linear dynamics at the collinear points is of the type centre×centre×saddle. In this section we focus on the effect that the nonlinear terms

have in this description. We first describe the method used, and then we will apply it to our situation.

Let us consider a Hamiltonian with three degrees of freedom, in a neighbourhood of an equilibrium point of the type centre×centre×saddle, that we will assume to be at the origin. Of course, this is an unstable equilibrium point but we are interested in the existence of trajectories that remain close to the point for all times. If we consider the linearization of the vectorfield at this point, and we skip the hyperbolic part, we obtain a couple of harmonic oscillators. Hence, for the linearized vectorfield, we have a couple of families of periodic orbits near the point, plus the quasiperiodic solutions obtained as product of the two families of periodic orbits. These quasiperiodic solutions are sometimes called Lissajous orbits [22]. Let us consider now the effect of the nonlinear terms of the vectorfield on these bounded solutions. Under generical conditions the well-known Lyapunov centre theorem says that, for each linear (periodic) oscillation, there exists a one-parametric family of periodic orbits of the complete Hamiltonian system that emanates from the point in a tangent way to the family of linear oscillations. The limit frequency of these periodic orbits at the fixed point is the frequency of the linear oscillations (see, for instance, [74, 60]). A similar result holds for the quasi-periodic Lissajous orbits: under general hypotheses, it can be shown that these linear oscillations can be extended to the complete system as a Cantorian two-parametric family of two-dimensional invariant tori. Moreover, the measure of the gaps between tori is exponentially small with the distance to the origin (for the proofs, see [48]).

In this section we will perform an effective computation of the dynamics near the collinear points, by means of the so-called reduction to the centre manifold. With this, we will be able to obtain an explicit representation of the bounded motions in an extended neighbourhood of the equilibrium point. As an example, we will do the computations for a concrete value of the mass parameter μ. These results are based on a combination of numerical and semi-analytical tools. Proofs for these results have to be computer assisted. For instance, see [13] to see the kind of work done in this direction.

Finally, let us mention that the results in this section can be extended beyond the radius of convergence of the power series used here, by means of purely numerical methods. See [41] for the details.

3.1   Reduction to the centre manifold

The process of reduction to the center manifold is very similar to a normal form calculation. It is based on removing all monomials involving p_1 or q_1 other than products p_1q_1 in the expansion of the Hamiltonian, to produce an invariant manifold tangent to the elliptic directions of H_2 (see Section 3.1.1 for details). Let us recall that, if $F(q,p)$ and $G(q,p)$ are two functions (where, as usual, q denotes the positions and p the momenta), their Poisson bracket is defined as

$$\{F,G\} = \frac{\partial F}{\partial q}\frac{\partial G}{\partial p} - \frac{\partial F}{\partial p}\frac{\partial G}{\partial q}.$$

In what follows, we will use the following notation. If $x = (x_1, \ldots, x_n)$ is a vector of complex numbers and $k = (k_1, \ldots, k_n)$ is an integer vector, we denote by x^k the value $x_1^{k_1} \cdots x_n^{k_n}$ (in this context we define 0^0 as 1). Moreover, we define $|k|$ as $\sum_j |k_j|$.

3.1.1 The Lie series method

Let us start by expanding the initial Hamiltonian around the equilibrium point, in the complex coordinates for which the second degree terms are in diagonal form (see Section 2.1). This expansion can be obtained by substituting the linear change obtained from the composition of (9) and (11) into the recurrence (5), that is then applied to compute the last sum in (3). The second degree terms in (3) that are not in the sum are obtained by direct substitution. In this way, the Hamiltonian takes the form

$$H(q,p) = H_2(q,p) + \sum_{n \geq 3} H_n(q,p), \tag{19}$$

where H_2 is given in (12) and H_n denotes an homogeneous polynomial of degree n with complex coefficients.

The changes of variables are implemented by means of the Lie series method: if $G(q,p)$ is a Hamiltonian system, then the function $\hat{H}$ defined by

$$\hat{H} \equiv H + \{H, G\} + \frac{1}{2!}\{\{H, G\}, G\} + \frac{1}{3!}\{\{\{H, G\}, G\}, G\} + \cdots, \tag{20}$$

is the result of applying a canonical change to H. This change is the time one flow corresponding to the Hamiltonian G. G is usually called the generating function of the transformation to obtain (20). See [31] and references therein for more details.

It is easy to check that, if P and Q are two homogeneous polynomials of degree r and s respectively, then $\{P, Q\}$ is a homogeneous polynomial of degree $r + s - 2$. This property is very useful to implement in a computer the transformation (20): for instance, let us assume that we want to eliminate the monomials of degree 3 of (19), as it is usually done in a normal form scheme. Let us select as a generating function a homogeneous polynomial of degree 3, G_3. Then, it is immediate to check that the terms of $\hat{H}$ satisfy

degree 2: $\hat{H}_2 = H_2$,

degree 3: $\hat{H}_3 = H_3 + \{H_2, G_3\}$,

degree 4: $\hat{H}_4 = H_4 + \{H_3, G_3\} + \frac{1}{2!}\{\{H_2, G_3\}, G_3\}$,

$\vdots$

Hence, to eliminate the monomials of degree 3 one has to look for a G_3 such that $\{H_2, G_3\} = -H_3$. Let us denote

$$H_3(q,p) = \sum_{|k_q|+|k_p|=3} h_{k_q,k_p} q^{k_q} p^{k_p}, \quad G_3(q,p) = \sum_{|k_q|+|k_p|=3} g_{k_q,k_p} q^{k_q} p^{k_p},$$

13

and $H_2(q,p) = \sum_{j=1}^{3} \eta_j q_j p_j$, where $\eta_1 = \lambda_1$, $\eta_2 = \sqrt{-1}\omega_1$ and $\eta_3 = \sqrt{-1}\omega_2$. As

$$\{H_2, G_3\} = \sum_{|k_q|+|k_p|=3} \langle k_p - k_q, \eta \rangle \, g_{k_q,k_p} q^{k_q} p^{k_p}, \quad \eta = (\eta_1, \eta_2, \eta_3),$$

it is immediate to obtain

$$G_3(q,p) = \sum_{|k_q|+|k_p|=3} \frac{-h_{k_q,k_p}}{\langle k_p - k_q, \eta \rangle} q^{k_q} p^{k_p},$$

that is well defined because the condition $|k_q| + |k_p| = 3$ implies that $\langle k_p - k_q, \eta \rangle$ is different from zero. Note that G_3 is so easily obtained because of the "diagonal" form of H_2 given in (12).

In this section we are not interested in a complete normal form, but only in un-coupling the central directions from the hyperbolic one. Hence, it is not necessary to cancel all the monomials in H_3 but only some of them. Moreover, as we want the radius of convergence of the transformed Hamiltonian to be as big as possible, we will try to choose the change of variables as close to the identity as possible. This means that we will eliminate the least possible number of monomials in the Hamiltonian. In order to produce an approximate first integral having the center manifold as a level surface (see below), it is enough to eliminate the monomials $q^{k_q} p^{k_p}$ such that the first component of k_q is different from the first component of k_p. This implies that the generating function G_3 is

$$G_3(q,p) = \sum_{(k_q,k_p) \in \mathcal{S}_3} \frac{-h_{k_q,k_p}}{\langle k_p - k_q, \eta \rangle} q^{k_q} p^{k_p}, \tag{21}$$

where $\mathcal{S}_n$, $n \geq 3$, is the set of indices (k_q, k_p) such that $|k_q| + |k_p| = n$ and the first component of k_q is different from the first component of k_p. Then, the transformed Hamiltonian $\hat{H}$ takes the form

$$\hat{H}(q,p) = H_2(q,p) + \hat{H}_3(q,p) + \hat{H}_4(q,p) + \cdots, \tag{22}$$

where $\hat{H}_3(q,p) \equiv \hat{H}_3(q_1 p_1, q_2, p_2, q_3, p_3)$ (note that $\hat{H}_3$ depends on the product $q_1 p_1$, not on each variable separately). This process can be carried out up to a finite order N, to obtain a Hamiltonian of the form

$$\bar{H}(q,p) = H_N(q,p) + R_{N+1}(q,p),$$

where $H_N(q,p) \equiv H_N(q_1 p_1, q_2, p_2, q_3, p_3)$ is a polynomial of degree N and R_{N+1} is a remainder of order $N+1$ (note that H_N depends on the product $q_1 p_1$ while the remainder depends on the two variables q_1 and p_1 separately). Neglecting the remainder (it is very small if we are close enough to the origin), we can define $I_1 = q_1 p_1$ (this is a canonical change if we define properly the corresponding angle variable) to obtain a Hamiltonian $H_N(I_1, q_2, q_3, p_2, p_3)$. Note that the equation corresponding to the variable I_1 is $\dot{I}_1 = 0$ so it is a first integral of the system. Selecting the value $I_1 = 0$ we are restricting the

14

Hamiltonian H_N to an invariant manifold that is tangent at the origin with the linear central part of the system. This is the so called reduction to the centre manifold. Finally, the Hamiltonian is put into its real form by using the inverse of (11).

Note that the normalizing method used here is slightly different than the one introduced in [19]. The main difference is that this process uses less computer memory, since it does not require to store the complete Lie triangle.

It is interesting to note the absence of small divisors during the entire process. The denominators that appear in the generating functions (like (21)), $\langle k_p - k_q, \eta \rangle$, can be bounded from below when $(k_q, k_p) \in \mathcal{S}_N$: using that η_1 is real and that $\eta_{2,3}$ are purely imaginary, we have

$$|\langle k_p - k_q, \eta \rangle| \geq |\lambda_1|, \quad \text{for all } (k_q, k_p) \in \mathcal{S}_N, \quad N \geq 3.$$

For this reason, the divergence of this process is very mild (the divergence of normalizing transformations in the absence of small divisors has been considered in other contexts, see, for instance, [7] or [9]; for a more general discussion see [65]). This is clearly observed when this process is stopped at some degree N. Then, the remainder is very small in a quite big neighborhood of the equilibrium point. We will deal with these points in the next section.

An explicit expression for the change of variables that goes from the coordinates of the center manifold to the coordinates corresponding to the Hamiltonian (19) can be obtained in the following way: once the generating function G_3 has been obtained, we can compute

$$\tilde{q}_j = q_j + \{q_j, G_3\} + \frac{1}{2!}\{\{q_j, G_3\}, G_3\} + \frac{1}{3!}\{\{\{q_j, G_3\}, G_3\}, G_3\} + \cdots, \quad (23)$$

$$\tilde{p}_j = p_j + \{p_j, G_3\} + \frac{1}{2!}\{\{p_j, G_3\}, G_3\} + \frac{1}{3!}\{\{\{p_j, G_3\}, G_3\}, G_3\} + \cdots, \quad (24)$$

that produces the transformation that sends the coordinates of (19), given by the variables $(\tilde{q}, \tilde{p})$ into the coordinates of (22), represented by the variables (q, p). In the next step, the generating function G_4 is applied to the right-hand side of equations (23) and (24), to obtain the change corresponding to fourth order, and so on.

Then, we perform the substitution $q_1 = p_1 = 0$ in the expressions for the change of variables, to obtain six power expansions (corresponding to the six initial variables), each one depending on the four variables of the center manifold. These expansions are put into real form in the same way as the Hamiltonian. From now on, and to simplify notation, the realified variables will still be called q and p.

We recall that, after replacing I_1 by 0, we have obtained a two degrees of freedom Hamiltonian system $H_c \equiv H_N(0, q_2, q_3, p_2, p_3)$, where the origin is an elliptic equilibrium point. It is not difficult to produce a qualitative description of the dynamics of H_c: the phase space is four dimensional, so let us fix an energy level $H_c = h_c$ to reduce to a three dimensional phase space. Now, Poincaré sections are two dimensional and can be plotted easily. Doing several plots for several values of h_c one gets a description of the trajectories that remain close to the origin. The dynamics of the initial Hamiltonian near the origin

can be obtained adding the hyperbolic part that we have skipped when reducing to the centre manifold. See [45] for further information.

Although the normalizing process used to approximate the center manifold is divergent in general, we can apply KAM techniques to show, under suitable hypotheses, the existence of a Cantorian centre manifold, completely filled up by invariant tori. This manifold is parametrized by two parameters (the actions of the tori), and each parameter moves on a Cantor set. The complementary of the measure of this manifold (in the parameters space) decreases exponentially with the distance to the origin. See [48] for more details. For a general discussion of the main features of centre manifolds, see [75] or [79].

3.1.2   The L_1 point of the Earth-Sun system

We have applied the above-explained algorithm to the collinear points of the RTBP. As a first example we have focused on the L_1 point corresponding to the mass parameter $\mu = 3.0404233984441761 \times 10^{-6}$. This is an approximate value for the Earth-Sun case. All the expansions have been performed up to degree $N = 32$.

The first terms of the Hamiltonian restricted to the center manifold are given in Table 1. The monomials that are not listed there have zero coefficient. In order to have an idea of the radius of convergence of this series, we have computed (numerically) the values

$$r_n^{(1)} = \frac{\|H_n\|_1}{\|H_{n-1}\|_1}, \quad r_n^{(2)} = \sqrt[n]{\|H_n\|_1}, \quad \text{where} \quad \|H_n\|_1 = \sum_{|k|=n} |h_k|, \quad 3 \le n \le N, \quad (25)$$

being h_k the coefficient of the monomial of exponent k. These values have been plotted in Figure 4. They seem to show a mild divergence of the series, although the region where the truncated series looks convergent (i.e., the region where the size of the last terms of the series is small) is quite big. Numerical and very realistic estimates of the radius of convergence are obtained as follows: take an initial condition inside the center manifold and, by means of a numerical integration of the reduced Hamiltonian, produce a sequence of points for the corresponding trajectory. Then, by means of the change of variables, send these points back to the initial RTBP coordinates. Finally, by means of a numerical integration of the RTBP, we can test if those points belong to the same orbit (note that we can not use a very long time span for those integrations, since the hyperbolic character of the center manifold in the RTBP amplifies the errors exponentially). This gives an idea of the error we have in the determination of the center manifold. In fact, the accuracy of the plots in Figures 3 and 6 has been checked in this way. For more details about this kind of error estimation, see [43].

To have a description of the dynamics inside the center manifold we use the following scheme: we take the 3D Poincaré section $q_3 = 0$ (this corresponds, at first order, to use $z = 0$ in the synodical coordinates) and we fix an energy level h_0 to obtain a 2D section. Hence, to obtain a picture of the phase space of this Poincaré section we select a value h_0 and an initial point (q_2, p_2). Using that $q_3 = 0$ and that the value of the Hamiltonian

16

k_1	k_2	k_3	k_4	h_k	k_1	k_2	k_3	k_4	h_k
2	0	0	0	1.0432267821115535e+00	0	0	2	2	1.2424817827573600e-01
0	2	0	0	1.0432267821115544e+00	4	1	0	0	-2.0023568581469642e-01
0	0	2	0	1.0076053314983200e+00	2	3	0	0	3.4353440405951968e-01
0	0	0	2	1.0076053314983200e+00	0	5	0	0	-2.0187593581785741e-02
2	1	0	0	6.5165140304211688e-01	2	1	2	0	-1.9849089558605101e-01
0	3	0	0	-4.1659670417917148e-02	0	3	2	0	1.4712780865620459e-01
0	1	2	0	5.3911539423589860e-01	0	1	4	0	-2.7451664895216100e-02
4	0	0	0	-8.5787309100706366e-02	3	0	1	1	-1.1415906236784655e-01
2	2	0	0	4.1161447802927803e-01	1	2	1	1	2.1573064571205472e-01
0	4	0	0	-2.6563655599297287e-02	1	0	3	1	-9.4058985172178297e-02
2	0	2	0	-1.4043712336878425e-01	2	1	0	2	1.9372724033920288e-01
0	2	2	0	2.7927960671292551e-01	0	3	0	2	-4.4040459096995777e-02
0	0	4	0	-5.7468618566454702e-02	0	1	2	2	1.9106055501181426e-01
1	1	1	1	6.2490402334472867e-02	1	0	1	3	3.8405228183256930e-02
2	0	0	2	1.5018398762952467e-01	0	1	0	4	-2.2759839111536957e-02
0	2	0	2	-2.8803507814853090e-02					

Table 1: Coefficients, up to degree 5, of the transformed Hamiltonian restricted to the center manifold corresponding to the L_1 point of the Earth-Sun system. The exponents (k_1, k_2, k_3, k_4) refer to the variables (q_2, p_2, q_3, p_3), in this order.

must be h_0, we compute (numerically) the corresponding value p_3 (in fact, there are two values that solve the equation, one positive and one negative; we use the positive one). Then, this point is used as an initial condition for a numerical integration of the Hamiltonian restricted to the central part, plotting a point each time that the trajectory crosses the plane $q_3 = 0$ with $p_3 > 0$.

The results can be seen in Figure 3. As the Hamiltonian is positive definite at the origin (this is clearly seen looking at the sign of the coefficients of the second degree terms in Table 1), each energy level defines a closed region in the Poincaré section. The boundary of this region coincides with a periodic orbit of the planar Lyapunov family of L_1, that is fully contained in the plane $q_3 = p_3 = 0$, and in the figure it has been plot using a continuous line. The motion inside this region is clearly quasi-periodic (except by some gaps that are too small to appear in these pictures), with a fixed point on the p_1 axis, that corresponds to a vertical Lyapunov orbit. If the value of the energy increases, one can see how the well known Halo orbits (see Section 3.2) are born, as a bifurcation of the planar Lyapunov family. Note that the Halo orbits are surrounded by 2D invariant tori (see also [39] and [40]). The boundary between the tori around the Halo orbit and the tori around the vertical Lyapunov orbit is a homoclinic trajectory of the planar Lyapunov orbit. Of course, the homoclinic trajectory that goes out from the orbit and the one that goes in do not generally coincide: they should intersect one each other with a very small angle. This phenomenon is known as splitting of separatrices. Finally, by sending those orbits to the RTBP coordinates, it is possible to see that the description provided by those plots is valid (and very accurate) up to a distance of L_1 a little bit bigger than 60% of the L_1-Earth distance.
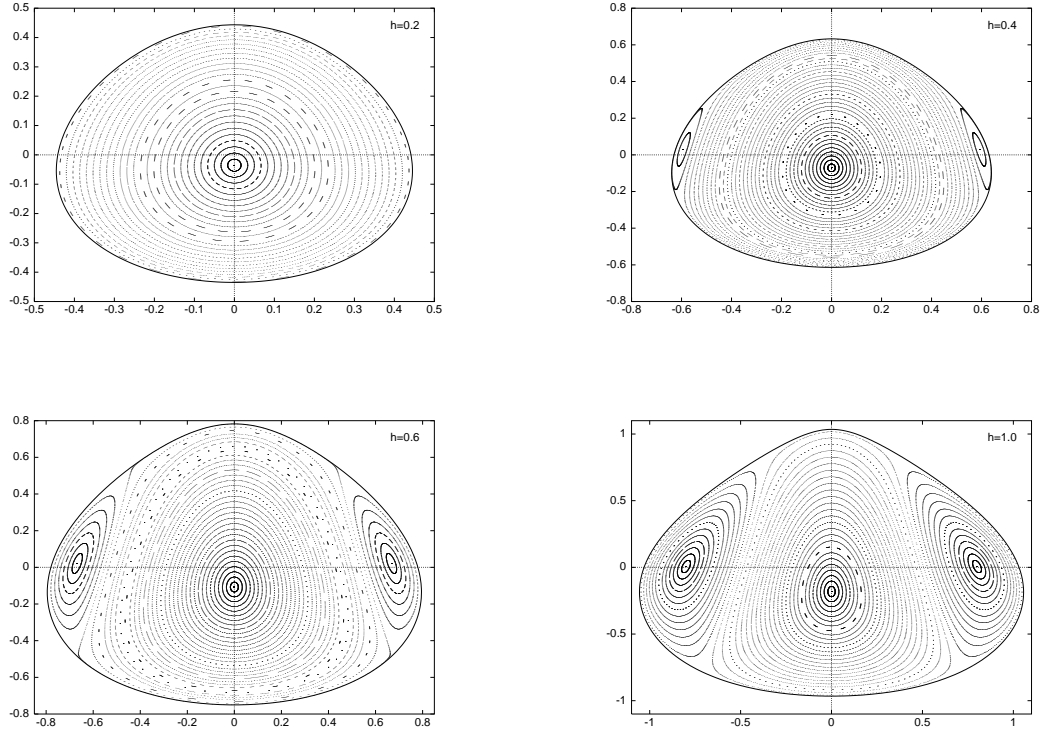
Figure 3: Poincaré sections of the center manifold of L_1, corresponding to $h = 0.2$, 0.4 0.6 and 1.0. Horizontal axis: q_2; vertical axis: p_2.

Figure 4: Horizontal axis: values of n. Vertical axis: the corresponding values of $r_n^{(1)}$ ($\Diamond$) and $r_n^{(2)}$ ($+$) according to (25), for the L_1 case.
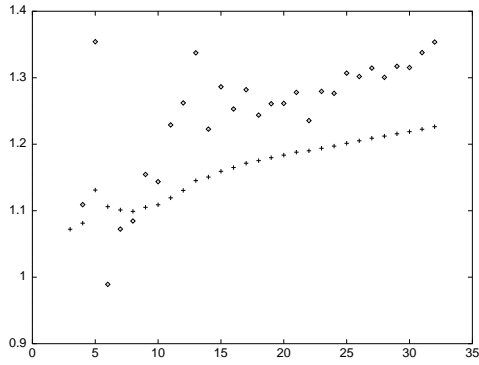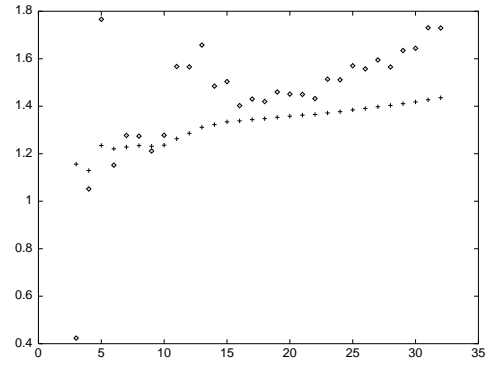
Figure 5: Horizontal axis: values of n. Vertical axis: the corresponding values of $r_n^{(1)}$ ($\Diamond$) and $r_n^{(2)}$ ($+$) according to (25), for the L_2 case.

k_1	k_2	k_3	k_4	h_k	k_1	k_2	k_3	k_4	h_k
2	0	0	0	9.3132294092164980e-01	0	0	2	2	1.6516656013507769e-01
0	2	0	0	9.3132294092164991e-01	4	1	0	0	3.0065634937222852e-01
0	0	2	0	8.9308808149867502e-01	2	3	0	0	-5.8388370855924443e-01
0	0	0	2	8.9308808149867525e-01	0	5	0	0	3.1707966658149511e-02
2	1	0	0	-8.3074621158508666e-01	2	1	2	0	2.4502956646982510e-01
0	3	0	0	6.5285116341699909e-02	0	3	2	0	-1.9424915041015245e-01
0	1	2	0	-6.4906335171207086e-01	0	1	4	0	8.2423593768551455e-03
4	0	0	0	-3.0986677967027330e-02	3	0	1	1	1.7854668840138077e-01
2	2	0	0	5.9388694902317307e-01	1	2	1	1	-4.2089157809945715e-01
0	4	0	0	-4.1582038336828324e-02	1	0	3	1	1.3900075305874218e-01
2	0	2	0	-4.7016550083469763e-02	2	1	0	2	-2.8565999503473249e-01
0	2	2	0	3.5694318621877408e-01	0	3	0	2	7.7193563104132376e-02
0	0	4	0	-1.7818840096908990e-02	0	1	2	2	-2.8562245235708378e-01
1	1	1	1	1.1056617867458479e-01	1	0	1	3	-7.5028466176853367e-02
2	0	0	2	2.1139923206390523e-01	0	1	0	4	4.3954249987303046e-02
0	2	0	2	-4.9839132339243322e-02					

Table 2: Coefficients, up to degree 5, of the Hamiltonian restricted to the center manifold corresponding to the L_2 point of the Earth-Moon system. The exponents (k_1, k_2, k_3, k_4) refer to the variables (q_2, p_2, q_3, p_3), in this order.

3.1.3   The L_2 point of the Earth-Moon system

It is not difficult to repeat the computations of the last section for the L_2 point of the Earth-Moon system. The Hamiltonian restricted to the center manifold is displayed in Table 2, and the estimates of the region of convergence are shown in Figure 5. Figure 6 contains the plots of the Poincaré sections, where the bifurcation that gives rise to the Halo orbits is also shown. As before, it is possible to check that this description is very accurate up to a half distance from L_2 to the Moon. As the results are very similar to the last case, we do not add further remarks.

3.1.4   The L_3 point of the Earth-Moon system

We have also performed these computations for the L_3 point. The main difference between this point and $L_{1,2}$ can be seen in Figure 1: while $L_{1,2}$ are strongly influenced by the two bodies, L_3 is influenced by the bigger primary but the effect of the smaller primary is almost neglectable. This implies that the dynamics near L_3 is rather close to the dynamics of a two body problem (which is very degenerate). This is the reason for the big coefficients shown in Table 3, that are responsible for the poor convergence radius shown in Figure 7: Hence, one must use very small values of the energy in order to be inside the region of convergence. This does not allow to go far enough to observe the bifurcation corresponding to the Halo orbits and, for this reason, we have not included the corresponding plots for this case.

So, the study of the behavior around L_3 (including the computation of Halo orbits) is a difficult problem. Moreover, as far as we know, there are no astronautical or as-
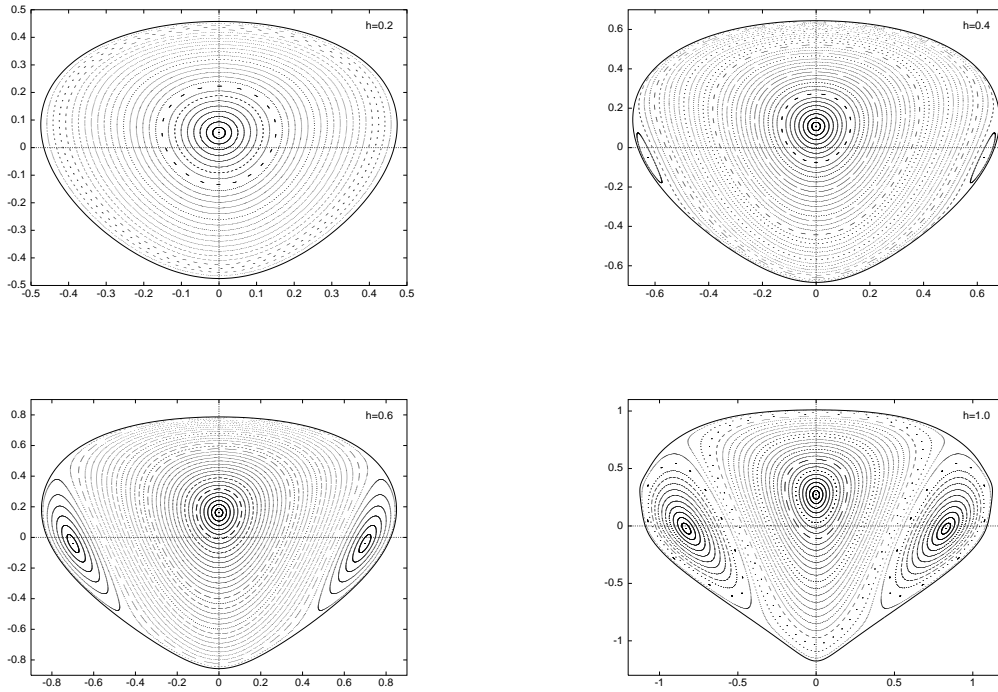
Figure 6: Poincaré sections of the center manifold of L_2, corresponding to $h = 0.2$, 0.4 0.6 and 1.0. Horizontal axis: q_2; vertical axis: p_2.

tronomical applications that require an accurate knowledge of the phase space around this point. We believe that, in case that this study were necessary, it would be better to look at it as a slightly perturbed two body problem rather than using the techniques discussed here.

3.2 Halo orbits

Halo orbits are periodic orbits which bifurcate from the planar Lyapunov periodic orbits when the in plane (or intrinsic) and out of plane (or normal) frequencies are equal. This is a 1:1 resonance that appear as a consequence of the nonlinear terms of the equations.

The importance of these orbits became clear with the mission ISEE 3 (it stands for International Sun-Earth Explorer) that was launched in 1978. The purpose of this probe was to study the Sun so it was desirable to place it in between Earth and Sun, to have a continuous monitoring of the activity of the Sun. Note that to place it at the L_1 point satisfies this requirement but with the following drawback: as seen from the Earth, the spacecraft would be in the middle of the Solar disk. This means that an antenna pointing to the probe is also pointing to the Sun, and the noise coming from the Sun would make it impossible to receive any data from the probe. Halo orbits provide a very good alternative to place the spacecraft: As seen from the Earth, a Halo orbit with low

k_1	k_2	k_3	k_4	h_k	k_1	k_2	k_3	k_4	h_k
2	0	0	0	5.0520994612145753e-01	0	0	2	2	7.1591406119636058e-01
0	2	0	0	5.0520994612145753e-01	4	1	0	0	2.1323011406157320e+03
0	0	2	0	5.0266571276387528e-01	2	3	0	0	-5.6249141438829110e+02
0	0	0	2	5.0266571276387528e-01	0	5	0	0	1.3204637130128873e+01
2	1	0	0	-5.6115912436382951e+00	2	1	2	0	5.2838311677563991e+02
0	3	0	0	9.3496383336128464e-01	0	3	2	0	-3.0623587048451135e+01
0	1	2	0	-1.4686056924068396e+00	0	1	4	0	1.5515423765627251e+01
4	0	0	0	7.6528931476095536e+00	3	0	1	1	1.8825389781246327e+00
2	2	0	0	1.3546730001510483e+01	1	2	1	1	-3.6872790343761423e+01
0	4	0	0	3.8069286794284551e-01	1	0	3	1	1.7599729630272192e+00
2	0	2	0	3.3499313360906959e+00	2	1	0	2	5.0848622203654816e+02
0	2	2	0	7.9659730977543119e-01	0	3	0	2	-2.9960960321274250e+01
0	0	4	0	3.5254807289843670e-01	0	1	2	2	2.7128291101879991e+01
1	1	1	1	4.0669264872473150e+00	1	0	1	3	-5.2867739300861096e+00
2	0	0	2	2.7355314621061146e+00	0	1	0	4	1.7913955620592070e+01
0	2	0	2	-1.3673249909233478e+00					

Table 3: Coefficients, up to degree 5, of the Hamiltonian restricted to the center manifold corresponding to the L_3 point of the Earth-Moon system. The exponents (k_1, k_2, k_3, k_4) refer to the variables (q_2, p_2, q_3, p_3), in this order.
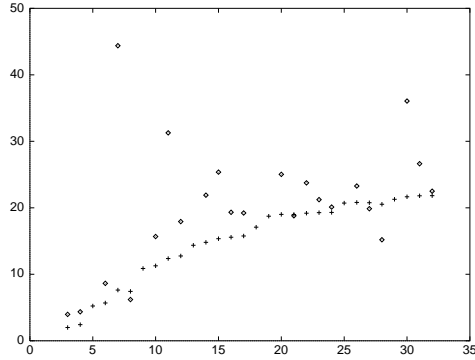

Figure 7: Horizontal axis: values of n. Vertical axis: the corresponding values of $r_n^{(1)}$ ($\Diamond$) and $r_n^{(2)}$ ($+$) according to (25), for the L_3 case.

21

vertical amplitude is seen as moving East and West through the Solar disk, but if the orbit is selected with a large enough vertical amplitude, the orbit is seen moving around the Solar disk, without crossing it. This is the reason for using the word "Halo" to name these these orbits: they somehow remind of a halo around a saint. Note that a probe on one of these orbits can keep permanent communications with the Earth while it has a continuous coverage of the Sun. Pioneer works in this direction are [22, 67] (Sun-Earth), [80] (Sun-Jupiter), and [10] (Earth-Moon).

3.3   Applications

As it has been mentioned in the previous section, Halo orbits have a natural interest in astrodynamics. The first mission using a Halo orbit was ISEE 3, launched in 1978. Since then many other missions have used these orbits as a suitable place

The quasi-periodic orbits near the collinear points have also been used in some missions. We mention the Herschel-Planck mission, that has put two satellites in a Lissajous orbit close to the L_2 point of the Earth-Sun system, to study the universe.

An interesting astronomical application can be found in [52], where the authors study the dynamics of some comets that have fast transitions from an orbit outside to that of Jupiter to an orbit that is inside, and viceversa. Examples of such comets are Oterma and Gehrels 3. The dynamical mechanism behind these transitions are the connections between neighbourhoods of L_1 and L_2 of the Sun-Jupiter system.

The use of the unstable component of the dynamics to connect different orbits near the collinear points is studied systematically in [12] with the idea of providing cheap transfers for an spacecraft moving close to one of the collinear points.

Another astronautical application is the so called "Petit Grand Tour" between the moons of Jupiter. This is design for a mission to visit the main moons of Jupiter, taking advantage of the different collinear points of the moons. See [53, 35] for the details.

4   Nonlinear dynamics near the triangular points

As it has been mentioned before, the Lagrangian points are linearly stable when μ is less than the Routh critical value μ_R. We will focus on this case.

The tools we will use in this section are similar to the ones in the previous sections. As it has been explained in Section 2.2, we can expand the Hamiltonian these points as

$$H(x, y) = H_2(x, y) + H_3(x, y) + H_4(x, y) + \cdots.$$

We have also seen that, in suitable real coordinates, H_2 takes the form

$$H_2(x, y) = \frac{1}{2}\omega_1(x_1^2 + y_1^2) + \frac{1}{2}\omega_2(x_2^2 + y_2^2) + \frac{1}{2}(x_3^2 + y_3^2).$$

So, in complex coordinates, it takes the form

$$H_2 = \sqrt{-1}\omega_1 q_1 p_1 + \sqrt{-1}\omega_2 q_2 p_2 + \sqrt{-1}q_3 p_3. \tag{26}$$

For the moment being, and to simplify the discussion, let us assume that the frequencies $(\omega_1, \omega_2, 1)$ are non-resonant.

4.1 Birkhoff normal form

Let us detail the computation of the normal form. We use Lie series, since they are very suitable to perform explicit computations, in a similar way it has been done in Section 3.1.1. The main difference is that now we try to eliminate all possible monomials in the expansion. As we did before, let us focus in the monomials of degree 3, after the first transformation,

$$H_3' = H_3 + \{H_2, G_3\}.$$

Hence, we ask $H_3' = 0$. This equation is easily solved, because H_2 is of the form (26): let us denote by k^q the three indices of k that correspond to the variable q and by k^p the ones of p. The expressions of H_3 and G_3 can be written as

$$H_3 = \sum_{|k|=3} h_3^k q^{k^q} p^{k^p}, \qquad G_3 = \sum_{|k|=3} g_3^k q^{k^q} p^{k^p}.$$

Hence, assuming that the frequencies $\omega = (\omega_1, \omega_2, 1)$ of H_2 are rationally independent, it is not difficult to obtain the coefficients g_3^k of G_3:

$$g_3^k = \frac{-h_3^k}{\sqrt{-1} \langle k^p - k^q, \omega \rangle}.$$

As in this case $|k|$ is 3 (odd), the denominator $\langle k^p - k^q, \omega \rangle$ is never zero. When dealing with even degrees (i.e., $|k|$ even), one must consider the case $k^p = k^q$ (note that, as the components of ω are rationally independent, this is the only possibility to produce a zero divisor). This implies that this monomial can not be eliminated and then we select the corresponding g_3^k equal to zero. Of course, if one wants to perform the normal form up to degree N, it is enough to ask $\langle k, \omega \rangle \neq 0$ when $0 < |k| < N$. If this condition is not satisfied we can still perform a resonant normal form, that is, we can eliminate all the monomials except the ones for which $\langle k, \omega \rangle = 0$ (usually called resonant monomials). Even when the frequencies are rationally independent, some of the denominators $\langle k, \omega \rangle$ can be very small, reducing drastically the domain where these transformations are valid. In this case is also possible to leave those monomials in the normal form, in order to keep a reasonable size for the domain of convergence (note that then the normal form might not be integrable, see [76] for a discussion of this technique). After a finite number of steps, the Hamiltonian takes the form

$$H(q, p) = H_2(q, p) + H_4(q, p) + H_6(q, p) + \cdots + H_{2N}(q, p) + R_{2N+1}(q, p),$$

where the homogeneous polynomials H_{2j} are in normal form, that is, they only contain monomials such that $k^p = k^q$. Terms of degree higher than $2N$ are not in normal form and they are all in the remainder R_{2N+1}.

The final step is to write the transformed Hamiltonian in real veriables. Let us start by using the inverse of the complexifying change,

$$q_j = \frac{x_j - \sqrt{-1}y_j}{\sqrt{2}}, \quad p_j = \frac{-\sqrt{-1}x_j + y_j}{\sqrt{2}}, \quad j = 1, 2, 3,$$

where we use q_1, q_2, q_3, p_1, p_2 and p_3 for x, y, z, p_x, p_y and p_z respectively. In order to put the Hamiltonian in the easiest possible form, we compose this change with

$$x_j = \sqrt{2I_j} \cos \phi_j, \quad y_j = -\sqrt{2I_j} \sin \phi_j, \quad j = 1, 2, 3.$$

This is equivalent to

$$q_j = I^{1/2} \exp(\sqrt{-1}\phi_j), \quad p_j = -\sqrt{-1}I^{1/2} \exp(-\sqrt{-1}\phi_j), \tag{27}$$

Hence, as the monomials that appear in the normal form have the same exponent both for positions and momenta ($k^q = k^p$ in the notation above), the change (27) makes them to depend only on the actions I_j:

$$h_k q^{k^q} p^{k^p} = h_k (\sqrt{-1})^{|k^q|} I^{k^q}.$$

Hence, the truncated Hamiltonian takes the form

$$H = H(I) = \langle \omega, I \rangle + \bar{H}_2(I) + \cdots + \bar{H}_N(I),$$

where $\bar{H}_j$ are homogeneous polynomials of degree j in the action variables I. This is now an integrable Hamiltonian, that can be used to give an approximate description of the dynamics around the equilibrium point.

4.1.1 Invariant tori

Let us use this normal form to give an approximate description of the dynamics close to an elliptic equilibrium point. This will help us later on to describe the effects of perturbations on this dynamics. If we neglect the remainder, the equations of motion are

$$\dot{I} = 0, \quad \dot{\phi} = \frac{\partial H(I)}{\partial I} = \bar{\omega}(I),$$

where ϕ is the vector of angles conjugated to the actions I. The solutions are $I(t) = I_0$ (that correspond to invariant tori) and $\phi(t) = \bar{\omega}(I_0)t + \phi_0$, that is a quasiperiodic flow on the torus.

Now let us recall that $I_j = \frac{1}{2}(x_j^2 + y_j^2)$, where (x, y) are the (real) variables of the normalized Hamiltonian. This means that, in order to have real (i.e., non complex) orbits, the actions I_j cannot be negative. In particular, if all the actions are zero, we are at the equilibrium point. The frequencies at the equilibrium point $I = 0$, $\bar{\omega}(0)$, are the frequencies of the linearisation at the point. To move away from the equilibrium point we have to increase the values of the actions and, as they can only have positive values,

we cannot achieve any frequency close to $\bar{\omega}(0)$ (in other words, having a diffeomorphism of an open set of frequencies around $\bar{\omega}(0)$ onto an open set of actions near $I = 0$ means to include negative values of the actions).

Assume now that only one action is strictly positive, say I_1. Then the trajectory is a periodic orbit whose frequency is the first component of $\bar{\omega}(I_1, 0, 0)$ (the other components are the normal frequencies of this periodic orbit). Of course, we can repeat this same reasoning for the other actions, giving rise to the families of Lyapunov periodic orbits around the point. If two actions are strictly positive, for instance I_1 and I_2, then the motion corresponds to a normally elliptic two dimensional torus whose frequencies are the first two components of $\bar{\omega}(I_1, I_2, 0)$. The third component of this vector is the normal frequency of the torus. In this case, these two tori (that sometimes are referred as Lyapunov lower dimensional tori) are parametrized by the two actions I_1 and I_2. Finally, when the three actions are strictly positive, we obtain the three dimensional tori around the point.

The effect of the remainder on this description can be shortly described as follows. The family of Lyapunov periodic orbits is not destroyed by the perturbation but only slightly deformed. This is the statement of the so-called Lyapunov center theorem that we have already mentioned in this chapter (see also [74, 60]). The effect of the remainder on the families of Lyapunov elliptic lower dimensional tori is more involved. It can be proved that, under generic conditions, most of these tori survive the effect of the remainder (see [48]). The structure of this set has a Cantorian structure, as it is usual in these situations. Finally, the effect of the remainder on the maximal (three in our case) dimensional tori is discussed by the classical KAM theorem (see [6]) and it will be discussed in the next sections.

4.2   On the stability

Assume that we have a Hamiltonian system with an elliptic equilibrium point (that we locate at the origin) of a $\ell > 1$ degrees of freedom autonomous Hamiltonian system $H(q, p)$. Consider an initial condition close to the origin. We are interested in knowing if the corresponding trajectory will be close to the origin for all times (stability in the sense of Lyapounov), or if it is going to escape to a distance $O(1)$ from the equilibrium point.

4.2.1   The Dirichlet theorem

This is a particular case in which the stability problem can be easily solved. Let us call M to the Hessian matrix of the Hamiltonian at the origin (we recall that M is symmetric and that $\nabla_{(q,p)}H(0, 0) = 0$). Assume that M is a positive definite matrix. Then, the Dirichlet theorem says that origin is Lyapounov stable.

The proof is based on the fact that, close to the point, the level surfaces of the Hamiltonian are "like ellipsoids" having the origin inside (those manifolds are of codimension 1 so they divide the phase space in two connected components). Then, as they

are invariant for the dynamics, they act as a barrier that the trajectories starting near the point cannot cross. Note that the same argument holds if there exists a first integral, defined on a neighbourhood of the origin, that is positive definite at $(0,0)$.

Unfortunately, there are many interesting cases where the matrix M is not positive definite (for instance, the $L_{4,5}$ points) and, hence, we need a different kind of results to study the stability.

4.2.2   KAM and Nekhoroshev theory

In Section 4.1 we have seen that, using a finite number of steps of a normal form scheme, we can put the Hamiltonian into the form

$$H = \langle \omega, I \rangle + \bar{H}_2(I) + \cdots + \bar{H}_N(I) + R_{N+1}. \tag{28}$$

Note that if the effect of the remainder would be neglectable, then we will obtain the Lyapunov stability of the equilibrium point: the dynamics of the integrable part reduces to quasi-periodic motions around the elliptic point. However, the effect of the remainder makes the problem much more difficult. Here we will focus in two ways of dealing with the effect of this remainder.

The first approach to deal with the remainder of (28) is to try to remove it completely. This cannot be done using the normal form scheme we have explained in the previous sections (the scheme is divergent), but it can be done through a Newton method. This is a quadratically convergent iterative scheme, introduced by A.N. Kolmogorov ([51]), to prove the preservation of tori with Diophantine frequencies. The ideas of Kolmogorov, jointly with the works by V.I. Arnol'd ([3]) and J. Moser ([62]) gave rise to the so called KAM theory, that deals with the existence and persistence of quasi-periodic motions in conservative systems (although some of these techniques have also been used in more general settings). One of the key points in this theory is to focus on tori with Diophantine frequencies. We recall that a vector of ℓ frequencies is called Diophantine if it satisfies

$$|\langle k, \omega \rangle| > \frac{c}{|k|^\gamma}, \quad c > 0, \quad k \in \mathbb{Z}^\ell \setminus \{0\}, \quad \gamma > \ell - 1,$$

where ℓ is the number of degrees of freedom (3 in our case). The set of Diophantine frequencies has empty interior but a large Lebesgue measure. This implies that the preserved tori fill a Cantor set of the phase space. On this Cantor set, the trajectories take place on invariant tori and, hence, they never go away from a vicinity of the origin. If we focus on the ball of radius r centered at the origin, the Lebesgue measure of the complementary of this Cantor set can be bounded by $c_1 \exp(-c_2(1/r)^{2/(\gamma+1)})$, $c_1 > 0$, $c_2 > 0$, for r small enough ([48]). This kind of results belongs to the so-called KAM theory. To decide about the stability we must take into account the motion outside the Cantor set of invariant tori. For instance, let us consider first the case of two degrees of freedom (this is the case of the planar RTBP). The phase space is four dimensional and, fixing the energy level $H = h$ we restrict to a three dimensional space. The invariant tori are of dimension 2 so they split the phase space and, hence, this allows to conclude

the Lyapounov stability of the elliptic point. The case of three degrees of freedom (the spatial RTBP) is much more difficult. The reason is the following: fixing the energy level produces a five dimensional invariant manifold and the invariant tori are three dimensional so they do not split phase space and we can not conclude stability. In fact, the stability of Hamiltonian systems with three or more degrees of freedom is today an open question. The more accepted conjecture says that they are, generically, unstable (see [4]). The instability mechanism is usually known as Arnol'd diffusion.

The second approach is based on deriving estimates on the size of R_{N+1} that are of the kind $c_1 \exp(-c_2(1/r)^{2/(\gamma+1)})$ ($c_1 > 0$, $c_2 > 0$). As before, r denotes the radius of the ball centered at the origin on which we take the norm of R_{N+1}, and it is assumed to be sufficiently small. This has been obtained optimizing the size of the remainder with respect to the degree up to which the normal form is obtained, for each value of r. From this bound on the remainder, it is not diffcult to obtain lower bounds on the diffusion time (i.e., the time to move away) around the point (these ideas were first introduced in [63]). For instance, if we call $T(r)$ to the time to go out from a ball of radius $2r$ starting in a ball of radius r, we have

$$T(r) \geq c_3 \exp\left(c_4 \left(\frac{1}{r} \right)^{\frac{2}{\gamma+1}} \right),$$

being c_3 and c_4 positive constants (to obtain this estimate, analyticity plays an essential role). Of course, this is not a proof of stability but a "bound on the unstability". These kind of estimates are what is usually called Nekhoroshev estimates.

It is outside the scope of this paper to give detailed explanations of these results. We refer to books like [5] or [6] for a general explanation, and to [15, 61, 48, 8, 27] for more concrete results. Another reference using these techniques but with a different formulation is [56].

An important remark on the planar case is the following: we have mentioned that the KAM theorem allows to prove the nonlinear stability of the planar RTBP near the triangular points. For this result to be true we need to construct the normal form up to degree 4 in the (p, q) variables (or degree 2 in the I variables), which is the minimum requirement to apply the KAM theorem (this is the so-called non-degeneracy condition). This construction can be done for all $0 < \mu < \mu_R$ except for two values, for which the points are unstable. The details can be found in [57].

4.2.3   First integrals

Another approach to bound the diffusion near an elliptic equilibrium point, without computing the normal form. The idea is based in the following fact: if we can compute as many first integrals in involution as the number of degrees of freedom, then the system will be integrable so we will have stability. Of course, the system we are considering (the spatial RTBP) is not integrable so these integrals do not exist. What we will do is to compute power expansions of formal integrals at the equilibrium point. Truncated to a finite order, these expansions are not exact integrals because they have a very small drift.

Bounding this drift we obtain a bound on the diffusion near the equilibrium points. Let us see it with a bit more of detail.

Again, let us consider the dynamics near an equilibrium point of a Hamiltonian system. To simplify the discussion, we will assume that the equilibrium point is at the origin and that it is of elliptic type. The case in which some directions are hyperbolic can be done in a very similar way.

As in the previous cases, let us assume that the Hamiltonian is expanded in power series, with H_2 in diagonal form (as in (26)). Let us denote by F the (wanted) first integral, that we will expand in power series around the origin as $F = \sum_{j \geq 2} F_j$, where F_j denotes a homogeneous polynomial of degree j. From the condition $\{H, F\} = 0$ it is immediate to obtain the following recurrence:

$$\{H_2, F_n\} = -\sum_{j=3}^{n} \{H_j, F_{n-j+2}\}. \tag{29}$$

Hence, due to the diagonal form of H_2, it is very easy to solve F_n in terms of $F_2, \ldots, F_{n-1}$, assuming the standard non resonant conditions on the frequencies of the point ([32]). We have seen (see Section 3.1.1) that the linear operator $G \in P_n \mapsto \{H_2, G\} \in P_n$ (here P_n denotes the space of homogeneous polynomials of degree n) is not bijective. Then it is possible that, if the right hand side of (29) contains resonant monomials, this equation can not be solved. There are several cases when it can be proved that such monomials never appear. See [15] for a discussion of this. Note that now, given a F_2, we can compute the following terms F_3, F_4 and so on.

As usual, the series $F = \sum_{j \geq 2} F_j$ is divergent. However, from its asymptotic character we can derive quasi-integrals of motion by simply truncating the series to finite order. This means that, if f_n denotes a quasi-integral and $(q(t), p(t))$ is an orbit of the Hamiltonian system H then,

$$\dot{f}_n(q(t), p(t)) = \{H, f_n\}(q(t), p(t))$$

Bounding the Poisson bracket of this formula in a neighbourhood of the elliptic point one can derive estimates on the diffusion time near the point. For an application of these techniques, see [76, 15]. See also [55] for an early construction of quasi-integrals, and [16, 21] for estimations on the rate of divergence.

5   Perturbations

The Restricted Three-Body Problem is a first (and useful) model for many real situation in astrodynamics. There are, of course, more complex models to produce accurate predictions for realistic situations. These models take into account effects that are not included in the RTBP, like the non-sphericity of the bodies, the presence of more masses, the Solar radiation pressure or relativistic effects. To study the dynamics close to the equilibrium points of the RTBP, the first (in order of relevance) effects are due to the eccentricity of the primaries and to the gravitational attraction of other bodies.
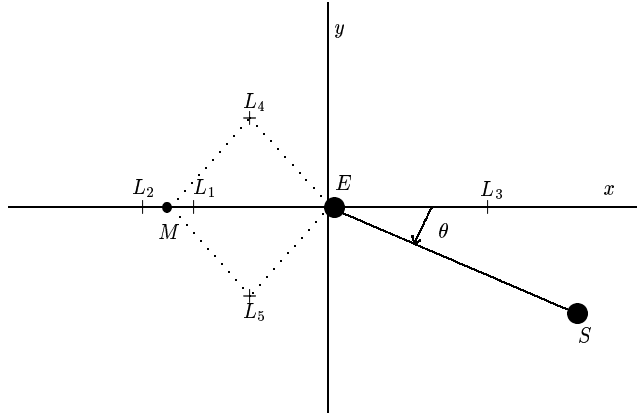
Figure 8: A schematic representation of the Bicircular problem.

5.1 Periodic time-dependent perturbations

There are several perturbations that are modelled as periodic time-dependent effects. Here we focus on the ones that are more relevant near the Lagrangian solutions.

5.1.1 The Elliptic Restricted Three-Body Problem

One of the first modifications to the RTBP is to assume that the motion of the primaries is not circular but elliptic, with some eccentricity $e \neq 0$. Then, the motion of an infinitesimal particle under the attraction of these primaries is what is known as the Elliptic Restricted Three-Body Problem. For the derivation of the equations of motion and of the basic properties, see [78].

The Elliptic RTBP has been studied extensively in the literature. The linear stability close to the triangular points has been studied in [18]. The nonlinear dynamics is usually studied using normal forms, as it has been explained in Section 4.1. For details, see [46, 54].

5.1.2 The Bicircular Problem

As far as we know, this model was first introduced in [17] to account for the direct effect of the Sun on a particle moving in the Earth-Moon RTBP. To introduce it, let us assume that Earth and Moon move in circular orbits (with constant angular velocity) around their common centre of mass, and that this centre of mass moves in a circular orbit (with constant angular velocity) around the Sun, that is fixed at the origin. Note that these bodies are not moving on a true solution of the Three-Body Problem.

It is very easy to write the vectorfield of an infinitesimal particle that moves under the gravitational attraction of these primaries, since the Sun is always at the origin and the positions of Earth and Moon are given by very simple trigonometric formulae. The study of the motion of this infinitessimal particle is what is called the Bicircular problem, BCP for short.

To simplify the model, it is usual to take the same units and reference frame as in the RTBP: Earth and Moon are sitting on the x axis as in Figure 1, while the Sun is turning around the origin in a circular way. Then, defining the momenta as $p_x = \dot{x} - y$, $p_y = \dot{y} + x$ and $p_z = \dot{z}$, it is not difficult to check that the motion of the infinitessimal particle is described by a Hamiltonian system that depends on time in a periodic way:

$$
\begin{aligned}
H_{BCP} &= \frac{1}{2}\left(p_x^2 + p_y^2 + p_z^2\right) + yp_x - xp_y - \\
&\quad -\frac{1-\mu}{r_{PE}} - \frac{\mu}{r_{PM}} - \frac{m_S}{r_{PS}} - \frac{m_S}{a_S^2}\left(y\sin\theta - x\cos\theta\right),
\end{aligned}
\tag{30}
$$

where $r_{PE}^2 = (x-\mu)^2 + y^2 + z^2$, $r_{PM}^2 = (x-\mu+1)^2 + y^2 + z^2$, $r_{PS}^2 = (x-x_S)^2 + (y-y_S)^2 + z^2$, $x_S = a_S\cos\theta$, $y_S = -a_S\sin\theta$, and $\theta = \omega_S t$. We stress that the BCP can be written as a periodic time dependent perturbation of the RTBP:

$$
H_{BCP}^\varepsilon = H_{RTBP} + \varepsilon\widehat{H}_{BCP}, \qquad \widehat{H}_{BCP} = -m_S\left(\frac{1}{r_{PS}} + \frac{y\sin\theta - x\cos\theta}{a_S^2}\right),
\tag{31}
$$

and it is clear that $H_{BCP}^{\varepsilon=0} = H_{RTBP}$, and that $H_{BCP}^{\varepsilon=1} = H_{BCP}$. The reason to add the parameter ε is that, near the Earth orbit, the effect of the Sun is quite large and should not be considered a perturbation. Hence, ε is more a continuation (homotopy) parameter rather than a perturbation one. For examples of the use of this model see [77, 14, 44].

The BCP is not only used to model the Earth-Moon-Sun system. For instance, it can be used to account for the direct effect of Saturn in the Sun-Jupiter RTBP. In this case the effect of Saturn in the neighbourhood of the orbit of Jupiter is small and can be considered as a perturbation.

5.1.3   The Bicircular Coherent Model

As it has been mentioned before, the Bicircular Coherent Problem (BCP) accounts for the direct effect of a third massive body on the infinitesimal particle of the RTBP model, but it does not include its effect on the two primaries. To simplify the explanations, let us assume that the massive bodies are Sun, Jupiter and Saturn. To derive a dynamically coherent model we need first to compute a periodic solution of the general Three-Body Problem, close to the real motion of Sun, Jupiter and Saturn. Although this is already a difficult problem, it can be solved by means of numerical methods. Once this periodic solutions has been obtained, it is not difficult to write the equations of motion for a particle under the gravitational attraction of these three bodies. Finally, using a suitable change of coordinates –in which Sun and Jupiter are kept fixed on the x-axis, as in the RTBP–, these equations of motion are written as a periodic time-dependent perturbation of the Sun-Jupiter RTBP.

This kind of model was first developed by M.A. Andreu and C. Simó to study the motion near the L_2 point of the Earth-Moon system taking into account the presence of the Sun (see [1, 2]). Later, it was also used to study the dynamics close to $L_{4,5}$ of the Sun-Jupiter system including the main effect of Saturn ([24]). A difference between these

two works is the method used to compute the periodic orbit for Sun, Earth and Moon. In [1, 2] this periodic orbit is obtained by means of a seminumerical method, while in [24] it is obtained using a shooting procedure.

5.2 Quasi-periodic models

In the previous section we have introduced some models that depend on time in a periodic way. A natural way of improving these models (to make them closer to reality) is to add more effects in the form of new time-dependent perturbations. The first models of this kind were developed in [36] to be used in the design of spacecraft missions near Libration points: among the applications we remark the design of a spacecraft mission to a Halo orbit close to the L_1 point of the Earth-Sun system.

Let us summarize how these models are derived. Assume, for instance, that we are interested in the dynamics near the triangular points of the Sun-Jupiter system, and that we are given a model for the motion of the main bodies of the Solar system (for instance, the JPL ephemeris). Then, we proceed with the following steps:

a) To write the vector field acting on a particle taking into account the gravitational attraction of Sun and planets.

b) Take coordinates such that Sun and Jupiter are kept fixed on the x axis. As in the RTBP, these coordinates are called synodical. Write the vector field defined in a) in these coordinates.

Now let us suppose that the particle is close to one of the equilibrium points of the Sun-Jupiter RTBP. In this situation, the vector field can be seen as a perturbation of the RTBP, with perturbing contributions coming from the real position of Sun and Jupiter and from the positions of the planets (note that this is not true if we are interested in the motion close to one of the primaries). Also note that for a model like the one given by the JPL ephemeris, there are no "simple closed formulas" for these positions. Next steps are:

c) Perform a frequency analysis on the perturbations (i.e., on the difference between this vectorfield and the RTBP vectorfield), and detect the dominant frequencies. As the motion of the Solar system seems to be quasi-periodic (at least for moderate time spans), it turns out that the part of these perturbing terms that depend on the positions of Sun and planets can be well approximated by trigonometric polynomials.

d) Substitute the dependence of the positions of the bodies by these truncated Fourier series.

e) The frequencies detected in c) can be written as a linear combination of a few of them, that correspond to the main frequencies of the motion of the bodies. We will refer to those as basic frequencies.

f) It is not necessary to take into account all the basic frequencies. In fact, the frequencies selected can be used as a control on the complexity (and the accuracy) of the model.

This technique has been used in [37, 33, 34]. Another reference about the derivation on these models close to Lagrangian solutions of some RTBP of the Solar system is [38]. These models have been used in some studies of the dynamics near the triangular points of Earth-Moon ([20]) and the Sun-Jupiter systems ([71, 28]).

5.3 The effect of periodic and quasi-periodic perturbations

In this section, we will first discuss the effect of periodic and quasi-periodic perturbations on an autonomous model in the neighbourhood of an equilibrium point of a differential equation, and then we will mention some of the implications for the Lagrangian solutions.

For the moment being, assume that we have an autonomous ODE with an equilibrium point at the origin plus a time-dependent quasi-periodic perturbation,

$$
\begin{aligned}
\dot{x} &= f(x) + \varepsilon g(x, \theta, \varepsilon), \\
\dot{\theta} &= \omega,
\end{aligned}
\tag{32}
$$

where $x \in \mathbb{R}^n$, $\theta \in \mathbb{T}^r$, $\omega \in \mathbb{T}^r$ and $f(0) = 0$. We also assume that the involved functions are analytic. It is known that, under standard non-resonance and non-degeneracy conditions, there exists a set $\mathcal{E}$ of values of ε such that:

- The set $\mathcal{E}$ is of large measure around $\varepsilon = 0$: if $m(\varepsilon)$ denotes the Lebesgue measure of the set $\mathcal{E} \cap [0, \varepsilon]$, then $\frac{m(\varepsilon)}{\varepsilon}$ is exponentially close (w.r.t. ε when ε goes to 0) to 1.

- For each $\varepsilon \in \mathcal{E}$, there exists a quasiperiodic solution of (32), with ω as vector of basic frequencies. The size of this solution is $O(\varepsilon)$, which means that this solution goes to the equilibrium point 0 when ε does.

For more details, see [47]. This result shows that the effect of the perturbation is to produce a quasi-periodic solution that "replaces" the equilibrium point. The set $\mathcal{E}$ has a Cantorian structure due to the resonances. For a detailed study of the effect of different resonances in a Hamiltonian setting, see [11].

To describe the nonlinear structure around this quasi-periodic solution we assume that (32) is a Hamiltonian vectorfield. Hence, the model can be described by means of a Hamiltonian function of the form

$$
H(q, p, \theta, I) = \langle \omega, I \rangle + H_0(p) + \varepsilon H_1(q, p, \theta, \varepsilon),
\tag{33}
$$

where θ denote the angles of the perturbation, ω its frequencies, I is the action corresponding to θ, and q and p are the angles and actions of the unperturbed Hamiltonian

H_0. The equations of motion are

$$\dot{q} = \frac{\partial H_0}{\partial p}(p) + \varepsilon \frac{\partial H_1}{\partial p}(q, p, \theta, \varepsilon),$$

$$\dot{p} = -\varepsilon \frac{\partial H_1}{\partial q}(q, p, \theta, \varepsilon),$$

$$\dot{\theta} = \omega.$$

We do not write the equation for the variable I, since it is an (artificial) action that has been added to obtain a Hamiltonian form. Its role is to compensate for the energy variations w.r.t. time such that Hamiltonian (33) is preserved, and it has no use in the description of the dynamics.

Strictly speaking, the Hamiltonian (33) does not satisfy the usual non-degeneracy condition (the frequencies ω do not depend on any action) so the standard KAM theorem cannot be applied. However, it is not difficult to see that the usual KAM proof works for this case, because there is no need to control the frequencies ω since they are not modified during the KAM iterations. Hence, for ε small enough, there exists an open set of (Diophantine) frequencies ν (these are frequencies coming from the unperturbed system H_0) such that (33) has invariant tori with frequencies (ω, ν). Of course, the Diophantine condition involves both the frequencies ω and ν. Again, for details see [47].

One can also ask for the persistence of other objects under quasi-periodic perturbations. For instance, we can think of the Lyapunov families of periodic orbits near the equilateral points (short period, long period and vertical), the Lissajous orbits near the collinear points or the well-known Halo orbits. In this direction, under generic non-resonance and non-degeneracy conditions, it is possible to prove the following results:

- Assume that the unperturbed system has a (smooth) family of periodic orbits. Then, under the effect of the quasi-periodic perturbation, this family becomes a Cantorian family of invariant tori. The basic frequencies of these tori are (ω, ν) where, as before, ω are the frequencies of the perturbation and $\nu \in \mathbb{R}$ denote the frequencies of the periodic orbits. The family becomes Cantorian because not all the frequencies ν are allowed, only those satisfying a suitable non-resonance condition.

- Assume that the unperturbed system has a (Cantor) family of lower dimensional tori. Examples can be the Lissajous orbits near the collinear points or near any equilibrium point with some center directions. Then, these families "add" the frequencies of the perturbation to their own set of frequencies $\nu \in \mathbb{R}^s$. Only those tori satisfying a non-resonance condition survive the perturbation.

Full details of these statements (including proofs) can be found in [49]. Examples of these situations can be seen in, for instance, [14].

These results can be summarized, in a crude way, saying that the effect of periodic or quasi-periodic time-dependent perturbations on the vicinity of the Lagrangian points is

to "shake" the dynamical structures that we have described for the (autonomous) RTBP: the equilibrium point becomes a periodic or quasi-periodic orbit, and the invariant tori around the point add the perturbing frequencies to the ones they already have. Of course, this needs that the perturbing frequencies and the frequencies of the torus are Diophantine. Hence, altough many tori are preserved, the measure of the surviving tori is reduced by the effect of the perturbation.

5.4   Other perturbations

There are other types of effects that can be relevant in specific situations. For instance, there is a growing interest in missions to asteroids, in which the effects of the nonspherical shape of the asteroid can be very relevant. In [29, 30] you can find a study of the dynamics close to the triangular points when one of the masses is an ellipsoid.

Another effect that can be relevant in some situations is the Solar radiation pressure. See [59] for the fundamentals and [23] to see how the tools of the previous sections apply to this situation.

5.5   The Solar system

As a first approximation, the Solar system can be seen as a collection of coupled two-body systems. This means that there are many situations for the motion of a spacecraft or an asteroid in which we have a perturbed restricted three-body problem.

A typical example of this situation is the Trojan motion. Classical studies use the RTBP model, but there are some works in which they use more realistic models. One of this models can be found in [25, 26], where the main perturbing planets are taken into account in the study the dynamics. Other studies using numerical integrations of the full system are [71, 70, 69, 72]. A numerical study on the existence of Trojan motions for a realistic model of the Earth-Moon system can be found in [44].

5.6   Applications to spacecraft dynamics

There are many astronautical missions that go to a vicinity of the collinear points of the Earth-Sun or Earth-Moon systems (those are the most common libration points used, but not the only ones).

The introduction of dynamical systems tools to the design of space missions to the neighbourhood of libration points started with [36], and continued with [37, 33, 34] Today, the use of tools such as invariant manifolds or heteroclinic connections starts to be very common. As example, we mention the the Genesis mission [58].

Acknowledgements

Related chapters

This chapter has a strong interaction with Chapter 12, "Space manifold dynamics", in this same volume.

References

[1] M.A. Andreu. *The quasi-bicircular problem*. PhD thesis, Univ. Barcelona, 1998.

[2] M.A. Andreu. Dynamics in the center manifold around L_2 in the quasi-bicircular problem. *Celestial Mech.*, 84(2):105–133, 2002.

[3] V.I. Arnold. Proof of A.N. Kolmogorov's theorem on the preservation of quasi-periodic motions under small perturbations of the Hamiltonian. *Russian Math. Surveys*, 18(5):9–36, 1963.

[4] V.I. Arnold. Instability of dynamical systems with several degrees of freedom. *Soviet Math. Dokl.*, 5:581–585, 1964.

[5] V.I. Arnold and A. Avez. *Ergodic Problems of Classical Mechanics*. Advanced Book Classics. Addison-Wesley, 1989.

[6] V.I. Arnold, V.V. Kozlov, and A.I. Neishtadt. *Dynamical Systems III*, volume 3 of *Encyclopaedia Math. Sci.* Springer, Berlin, 1988.

[7] A. Bazzani, M. Giovannozzi, G. Servizi, E. Todesco, and G. Turchetti. Resonant normal forms, interpolating Hamiltonians and stability analysis of area preserving maps. *Phys. D*, 64(1-3):66–97, 1993.

[8] G. Benettin, F. Fassò, and M. Guzzo. Nekhoroshev-stability of L_4 and L_5 in the spatial Restricted Three-Body Problem. *Regul. Chaotic Dyn.*, 3(3):56–72, 1998.

[9] G. Benettin and A. Giorgilli. On the Hamiltonian interpolation of near-to-the-identity symplectic mappings with application to symplectic integration algorithms. *J. Statist. Phys.*, 74(5-6):1117–1143, 1994.

[10] J.V. Breakwell and J.V. Brown. The 'Halo' family of 3-dimensional periodic orbits in the Earth-Moon restricted 3-body problem. *Celestial Mech.*, 20(4):389–404, 1979.

[11] H.W. Broer, H. Hanßmann, À. Jorba, J. Villanueva, and F.O.O. Wagener. Normal-internal resonances in quasiperiodically forced oscillators: a conservative approach. *Nonlinearity*, 16:1751–1791, 2003.

[12] E. Canalias, A. Delshams, J.J. Masdemont, and P. Roldán. The scattering map in the planar restricted three body problem. *Celestial Mech.*, 95(1-4):155–171, 2006.

[13] M.J. Capiński and P. Roldán. Existence of a Center Manifold in a Practical Domain around L_1 in the Restricted Three-Body Problem. *SIAM J. Appl. Dyn. Syst.*, 11(1):285–318, 2012.

[14] E. Castellà and À. Jorba. On the vertical families of two-dimensional tori near the triangular points of the Bicircular problem. *Celestial Mech.*, 76(1):35–54, 2000.

[15] A. Celletti and A. Giorgilli. On the stability of the Lagrangian points in the spatial Restricted Three Body Problem. *Celestial Mech.*, 50(1):31–58, 1991.

[16] G. Contopoulos, C. Efthymiopoulos, and A. Giorgilli. Non-convergence of formal integrals of motion. *J. Phys. A*, 36(32):8639–8660, 2003.

[17] J. Cronin, P.B. Richards, and L.H. Russell. Some periodic solutions of a four-body problem. *Icarus*, 3:423–428, 1964.

[18] J.M.A. Danby. Stability of the triangular points in the elliptic restricted problem of three bodies. *Astron. J.*, 69:165–172, 1964.

[19] A. Deprit. Canonical transformations depending on a small parameter. *Celestial Mech.*, 1:12–30, 1969/1970.

[20] C. Díez, À. Jorba, and C. Simó. A dynamical equivalent to the equilateral libration points of the real Earth-Moon system. *Celestial Mech.*, 50(1):13–29, 1991.

[21] C. Efthymiopoulos, A. Giorgilli, and G. Contopoulos. Nonconvergence of formal integrals. II. Improved estimates for the optimal order of truncation. *J. Phys. A*, 37(45):10831–10858, 2004.

[22] R.W. Farquhar and A.A. Kamel. Quasi-periodic orbits about the translunar libration point. *Celestial Mech.*, 7(4):458–473, 1973.

[23] A. Farrés and À. Jorba. Periodic and quasi-periodic motions of a solar sail close to SL_1 in the Earth-Sun system. *Celestial Mech.*, 107(1-2):233–253, 2010.

[24] F. Gabern and À. Jorba. A restricted four-body model for the dynamics near the Lagrangian points of the Sun-Jupiter system. *Discrete Contin. Dyn. Syst. Ser. B*, 1(2):143–182, 2001.

[25] F. Gabern and À. Jorba. Generalizing the Restricted Three-Body Problem. The Bianular and Tricircular Coherent Problems. *Astron. Astrophys.*, 420:751–762, 2004.

[26] F. Gabern and À. Jorba. Effective computation of the dynamics around a two-dimensional torus of a Hamiltonian system. *J. Nonlinear Sci.*, 15(3), 2005.

[27] F. Gabern, À. Jorba, and U. Locatelli. On the construction of the Kolmogorov normal form for the Trojan asteroids. *Nonlinearity*, 18(4):1705–1734, 2005.

[28] F. Gabern, À. Jorba, and P. Robutel. On the accuracy of restricted three-body models for the Trojan motion. *Discrete Contin. Dyn. Syst. Ser. B*, 11(4):843–854, 2004.

[29] F. Gabern, W.S. Koon, and J.E. Marsden. Spacecraft dynamics near a binary asteroid. *Discrete Contin. Dyn. Syst. Ser. A*, suppl.:297–306, 2005.

[30] F. Gabern, W.S. Koon, J.E. Marsden, and D.J. Scheeres. Binary asteroid observation orbits from a global dynamical perspective. *SIAM J. Appl. Dyn. Syst.*, 5(2):252–279, 2006.

[31] A. Giorgilli, A. Delshams, E. Fontich, L. Galgani, and C. Simó. Effective stability for a Hamiltonian system near an elliptic equilibrium point, with an application to the restricted three body problem. *J. Differential Equations*, 77:167–198, 1989.

[32] A. Giorgilli and L. Galgani. Formal integrals for an autonomous Hamiltonian system near an equilibrium point. *Celestial Mech.*, 17:267–280, 1978.

[33] G. Gómez, À. Jorba, J. Masdemont, and C. Simó. Study refinement of semi-analytical Halo orbit theory. ESOC contract 8625/89/D/MD(SC), final report, European Space Agency, 1991. Reprinted as *Dynamics and mission design near libration points. Vol. III, Advanced methods for collinear points*, volume 4 of World Scientific Monograph Series in Mathematics, 2001.

[34] G. Gómez, À. Jorba, J. Masdemont, and C. Simó. Study of Poincaré maps for orbits near Lagrangian points. ESOC contract 9711/91/D/IM(SC), final report, European Space Agency, 1993. Reprinted as *Dynamics and mission design near libration points. Vol. IV, Advanced methods for triangular points*, volume 5 of World Scientific Monograph Series in Mathematics, 2001.

[35] G. Gómez, W.S. Koon, M.W. Lo, J.E. Marsden, J. Masdemont, and S.D. Ross. Connecting orbits and invariant manifolds in the spatial restricted three-body problem. *Nonlinearity*, 17(5):1571–1606, 2004.

[36] G. Gómez, J. Llibre, R. Martínez, and C. Simó. Station keeping of libration point orbits. ESOC contract 5648/83/D/JS(SC), final report, European Space Agency, 1985. Reprinted as *Dynamics and mission design near libration points. Vol. I, Fundamentals: the case of collinear libration points*, volume 2 of World Scientific Monograph Series in Mathematics, 2001.

[37] G. Gómez, J. Llibre, R. Martínez, and C. Simó. Study on orbits near the triangular libration points in the perturbed Restricted Three–Body Problem. ESOC contract 6139/84/D/JS(SC), final report, European Space Agency, 1987. Reprinted

as *Dynamics and mission design near libration points. Vol. II, Fundamentals: the case of triangular libration points*, volume 3 of World Scientific Monograph Series in Mathematics, 2001.

[38] G. Gómez, J.J. Masdemont, and J.M. Mondelo. Solar system models with a selected set of frequencies. *Astron. Astrophys.*, 390(2):733–749, 2002.

[39] G. Gómez, J.J. Masdemont, and Simó S. Lissajous orbits around halo orbits. *Adv. in the Astronautical Sciences*, 95:117–134, 1997.

[40] G. Gómez, J.J. Masdemont, and C. Simó. Quasihalo orbits associated with libration points. *J. Astronaut. Sci.*, 46(2):135–176, 1998.

[41] G. Gómez and J.M. Mondelo. The dynamics around the collinear equilibrium points of the RTBP. *Phys. D*, 157(4):283–321, 2001.

[42] J. Henrard and J.F. Navarro. Families of periodic orbits emanating from homoclinic orbits in the restricted problem of three bodies. *Celestial Mech.*, 89(3):285–304, 2004.

[43] À. Jorba. A methodology for the numerical computation of normal forms, centre manifolds and first integrals of Hamiltonian systems. *Exp. Math.*, 8(2):155–195, 1999.

[44] À. Jorba. A numerical study on the existence of stable motions near the triangular points of the real Earth-Moon system. *Astron. Astrophys.*, 364(1):327–338, 2000.

[45] À. Jorba and J. Masdemont. Dynamics in the centre manifold of the collinear points of the Restricted Three Body Problem. *Phys. D*, 132:189–213, 1999.

[46] À. Jorba and C. Simó. Effective stability for periodically perturbed Hamiltonian systems. In J. Seimenis, editor, *Hamiltonian Mechanics: Integrability and Chaotic Behaviour*, volume 331 of *NATO Adv. Sci. Inst. Ser. B Phys.*, pages 245–252. Held in Toruń, Polland, 28 June–2 July 1993. Plenum, New York, 1994.

[47] À. Jorba and C. Simó. On quasiperiodic perturbations of elliptic equilibrium points. *SIAM J. Math. Anal.*, 27(6):1704–1737, 1996.

[48] À. Jorba and J. Villanueva. On the normal behaviour of partially elliptic lower dimensional tori of Hamiltonian systems. *Nonlinearity*, 10:783–822, 1997.

[49] À. Jorba and J. Villanueva. On the persistence of lower dimensional invariant tori under quasi-periodic perturbations. *J. Nonlinear Sci.*, 7:427–473, 1997.

[50] À. Jorba and J. Villanueva. Numerical computation of normal forms around some periodic orbits of the Restricted Three Body Problem. *Phys. D*, 114(3-4):197–229, 1998.

[51] A.N. Kolmogorov. On the persistence of conditionally periodic motions under a small change of the Hamilton function. *Dokl. Acad. Nauk. SSSR*, 98(4):527–530, 1954.

[52] W.S. Koon, M.W. Lo, J.E. Marsden, and S.D. Ross. Resonance and capture of Jupiter comets. *Celestial Mech.*, 81(1-2):27–38, 2001.

[53] W.S. Koon, J.E. Marsden, S.D. Ross, and M.W. Lo. Constructing a low energy transfer between Jovian moons. In *Celestial mechanics (Evanston, IL, 1999)*, volume 292 of *Contemp. Math.*, pages 129–145. Amer. Math. Soc., Providence, RI, 2002.

[54] Ch. Lhotka, C. Efthymiopoulos, and R. Dvorak. Nekhoroshev stability at L_4 or L_5 in the elliptic-restricted three-body problem – application to Trojan asteroids. *Mon. Not. R. Astron. Soc.*, 384(3):1165–1177, 2008.

[55] C. Marchal. The quasi integrals. *Celestial Mech.*, 21:183–191, 1980.

[56] C. Marchal. Long term evolution of quasi-circular Trojan orbits. *Celestial Mech.*, 104(1-2):53–67, 2009.

[57] A.P. Markeev. On the stability of the triangular libration points in the circular bounded three-body problem. *J. Appl. Math. Mech.*, 33:105–110, 1969.

[58] J.E. Marsden and S.D. Ross. New methods in celestial mechanics and mission design. *Bull. Amer. Math. Soc. (N.S.)*, 43(1):43–73, 2006.

[59] C.R. McInnes. *Solar Sailing: Technology, Dynamics and Mission Applications.* Springer-Praxis, 1999.

[60] K.R. Meyer and G.R. Hall. *Introduction to Hamiltonian Dynamical Systems and the N-Body Problem.* Springer, New York, 1992.

[61] A. Morbidelli and A. Giorgilli. On a connection between KAM and Nekhoroshev theorem. *Phys. D*, 86(3):514–516, 1995.

[62] J. Moser. On invariant curves of area-preserving mappings of an annulus. *Nachr. Akad. Wiss. Göttingen Math.-Phys. Kl. II*, 2:1–20, 1962.

[63] N.N. Nekhoroshev. An exponential estimate of the time of stability of nearly-integrable Hamiltonian systems. *Russian Math. Surveys*, 32:1–65, 1977.

[64] M. Ollé, J.R. Pacha, and J. Villanueva. Motion close to the Hopf bifurcation of the vertical family of periodic orbits of L_4. *Celestial Mech.*, 90(1-2):89–109, 2004.

[65] R. Pérez-Marco. Convergence or generic divergence of the Birkhoff normal form. *Ann. of Math. (2)*, 157(2):557–574, 2003.

[66] A.D. Pinotsis. Infinite Feigenbaum sequences and spirals in the vicinity of the Lagrangian periodic solutions. *Celestial Mech.*, 108(2):187–202, 2010.

[67] D.L. Richardson. Analytic construction of periodic orbits about the collinear points. *Celestial Mech.*, 22(3):241–253, 1980.

[68] D.L. Richardson. A note on a Lagrangian formulation for motion about the collinear points. *Celestial Mech.*, 22(3):231–236, 1980.

[69] P. Robutel and J. Bodossian. The resonant structure of Jupiter's Trojan asteroids – II. What happens for different configurations of the planetary system. *Mon. Not. R. Astron. Soc.*, 399:69–87, 2009.

[70] P. Robutel and F. Gabern. The resonant structure of Jupiter's Trojan asteroids – I. Long-term stability and diffusion. *Mon. Not. R. Astron. Soc.*, 372:1463–1482, 2006.

[71] P. Robutel, F. Gabern, and A. Jorba. The observed Trojans and the global dynamics around the Lagrangian points of the Sun-Jupiter system. *Celestial Mech.*, 92(1-3):53–69, 2005.

[72] P. Robutel and J. Souchay. An introduction to the dynamics of Trojan asteroids. In J. Souchay and R. Dvorak, editors, *Dynamics of Small Solar System Bodies and Exoplanets*, volume 790 of *Lect. Notes Phys.*, pages 195–227. Springer, 2010.

[73] B. Sicardy. Stability of the triangular Lagrange points beyond Gascheau's value. *Celestial Mech.*, 107(1-2):145–155, 2010.

[74] C. L. Siegel and J. K. Moser. *Lectures on Celestial Mechanics*, volume 187 of *Grundlehren Math. Wiss.* Springer, New York, 1971.

[75] J. Sijbrand. Properties of center manifolds. *Trans. Amer. Math. Soc.*, 289(2):431–469, 1985.

[76] C. Simó. Estabilitat de sistemes Hamiltonians. *Mem. Real Acad. Cienc. Artes Barcelona*, 48(7):303–348, 1989.

[77] C. Simó, G. Gómez, À. Jorba, and J. Masdemont. The Bicircular model near the triangular libration points of the RTBP. In A.E. Roy and B.A. Steves, editors, *From Newton to Chaos*, pages 343–370, New York, 1995. Plenum Press.

[78] V. Szebehely. *Theory of Orbits.* Academic Press, 1967.

[79] A. Vanderbauwhede. Centre manifolds, normal forms and elementary bifurcations. In *Dynamics reported, Vol. 2*, volume 2 of *Dynam. Report. Ser. Dynam. Systems Appl.*, pages 89–169. Wiley, Chichester, 1989.

[80] C.G. Zagouras and P.G. Kazantzis. Three-dimensional periodic oscillations generating from plane periodic ones around the collinear Lagrangian points. *Astrophys. Space Sci.*, 61:389–409, 1979.